Quarterly Reviews of Biophysics **39**, 4 (2006), pp. 361–396. © 2006 Cambridge University Press
doi:10.1017/S0033583506004458 Printed in the United Kingdom

The structure of aquaporins

Tamir Gonen[1]* and Thomas Walz[2]*

[1] Department of Biochemistry, University of Washington, Seattle, WA, USA
[2] Department of Cell Biology, Harvard Medical School, Boston, MA, USA

Abstract. The ubiquitous members of the aquaporin (AQP) family form transmembrane pores that are either exclusive for water (aquaporins) or are also permeable for other small neutral solutes such as glycerol (aquaglyceroporins). The purpose of this review is to provide an overview of our current knowledge of AQP structures and to describe the structural features that define the function of these membrane pores. The review will discuss the mechanisms governing water conduction, proton exclusion and substrate specificity, and how the pore permeability is regulated in different members of the AQP family.

* Correspondence may be addressed to either author:
T. Gonen – Tel.: (206) 616-7565, Fax: (206) 685-1792, Email: tgonen@u.washington.edu
T. Walz – Tel: (617) 432-4090, Fax: (617) 432-1144, Email: twalz@hms.harvard.edu

1. Introduction

Cells are surrounded by biological membranes that separate the cell's interior from the outside world. These lipid bilayers are vital for the structural integrity of cells, and the proteins embedded in the lipid bilayer are responsible for sensing the outside world, for the controlled exchange of substances between the cell and its environment, and for maintaining electrochemical gradients that provide the energy for many physiological processes. Most of the interior of a cell is water, which can diffuse freely through the lipid bilayer, but only at a limited rate. For many years it has been known, however, that some cells exhibit a much higher water permeability than others, prompting the hypothesis that specialized proteins may exist that facilitate the conduction of water across biological membranes (Sidel & Solomon, 1957). It took several decades until these postulated water pores were finally identified.

1.1 The elusive water pores

In the 1960s it was shown that amphibian skin epithelia display a very high water permeability (Ussing, 1965) and that red blood cells exhibit large selective water conductance with low Arrhenius activation energy (Rich *et al.* 1968). The water permeability of red blood cells was selectively inhibited by $HgCl_2$ and could be restored by treating the cells with reducing agents (Macey, 1984). This led to the realization that red blood cell membranes must have proteins that act as water pores and contain free sulfhydryl groups that can react with mercurials. Since it was thought at the time that all red blood cell membrane proteins had been identified, it was assumed that one of the known membrane proteins would also harbor the water pore function. Various approaches were taken to identify the postulated water pore. In an attempt to label the water pores, red blood cell membranes were exposed to isotopic mercury but this approach failed to identify the protein (Solomon *et al.* 1983). Glucose transporter 1, an early candidate to be the red blood cell water pore, was expressed in *Xenopus* oocytes, but the protein could not account for the high water conductance observed in red blood cells (Fischbarg *et al.* 1990). Functional studies on a number of other proteins also failed to demonstrate water pore function (Harris *et al.* 1992). Expression of mRNA isolated from kidney and red blood cells in oocytes resulted in a marked increase in water permeability, but yet again the identity of the water pore remained elusive (Zhang *et al.* 1990). It was serendipity that in the end led to the identification of the long sought-after red blood cell water pore.

1.2 CHIP28

The first water pore was identified by Peter Agre's group as part of ongoing work on the Rh(D) antigen. A diffuse protein band that migrated on SDS–PAGE gels at an apparent molecular weight of 30–32 kDa, previously thought to be a degradation product of the Rh protein, failed to cross-react with a polyclonal antibody against Rh. Further characterization established that the

gel band contained a novel red blood cell membrane protein that previously escaped detection, because of its failure to stain with Coomassie Blue. The newly discovered protein was found to be highly abundant and to exist as an oligomer, and it was thought to function as a channel. The protein was thus termed CHannel-forming Integral Protein of 28 kDa or 'CHIP28' (Agre *et al.* 1987). Sequence analysis revealed that CHIP28 belonged to the MIP family, named after the Major Intrinsic Protein from the lens fiber cell (Gorin *et al.* 1984), a seemingly heterogeneous group of membrane proteins with largely unknown functions (Pao *et al.* 1991).

In a breakthrough experiment using the *Xenopus* oocyte expression system, Agre and co-workers were able to demonstrate that CHIP28 was the postulated red blood cell water pore (Preston *et al.* 1992). Shortly after establishing the water pore function of CHIP28, homologous proteins in mammals, bacteria and plants were also shown to function as water pores, and the term 'aquaporin' was coined as a descriptive name for members of this protein family (Agre *et al.* 1993). Accordingly, CHIP28 was renamed to AQP1 and MIP is now known as AQP0.

Since the discovery of AQPs, many reviews have been written, providing accounts on the progress of our knowledge on various aspects of these proteins. Since several new AQP structures have been published in the last 2 years, the purpose of this review is to summarize our current knowledge of AQP structures, and to discuss their implications on the function and regulation of these proteins. We will only consider AQPs with currently known atomic structure. These are red blood cell AQP1 (Murata *et al.* 2000; Ren *et al.* 2001; Sui *et al.* 2001), *E. coli* glycerol facilitator GlpF (Fu *et al.* 2000; Tajkhorshid *et al.* 2002), *E. coli* water pore AQPZ (Savage *et al.* 2003; Jiang *et al.* 2006), eye lens-specific AQP0 (Gonen *et al.* 2004a, 2005; Harries *et al.* 2004), archaebacterial AQPM (Lee *et al.* 2005), plant SoPIP2;1 (Tornroth-Horsefield *et al.* 2006), and AQP4, the predominant water pore in brain (Hiroaki *et al.* 2006). This review will not discuss the structures of AQPs that are currently only known at low or intermediate resolution.

2. Studies on AQP1

Once AQP1 was shown to be a water pore, studies began towards elucidating its structure, pore properties, and the mechanisms underlying selective water conduction and proton exclusion.

2.1 Expression of AQP1 cDNA in *Xenopus* oocytes

Injection of AQP1 mRNA into *Xenopus* oocytes resulted in a dramatic increase in water permeability (Preston *et al.* 1992). Oocytes expressing AQP1 and control oocytes were transferred from isotonic modified Barth's solution of 200 mosmM to a diluted solution of only 70 mosmM. A significant increase in water permeability was observed in oocytes expressing AQP1 resulting in dramatic swelling followed by explosion of the oocytes, while control oocytes remained virtually unchanged (Fig. 1). $HgCl_2$ was known to inhibit water permeability of red blood cells (Macey, 1984), and swelling of AQP1-expressing oocytes could also reversibly be inhibited by the addition of $HgCl_2$, demonstrating that AQP1 was indeed the red blood cell water pore (Preston *et al.* 1992). Mutational analysis identified Cys189 to have the free sulfhydryl group that reacts with mercurials causing blockage of the pore (Zhang *et al.* 1993a). Furthermore, mutation of Cys189 to a larger, more hydrophobic tryptophan residue resulted in lower water permeability through AQP1 (Zhang *et al.* 1993a). AQP1 forms tetramers, in which only one or two monomers are glycosylated (Smith & Agre, 1991). Mutation of the glycosylation site Asn42 to a threonine

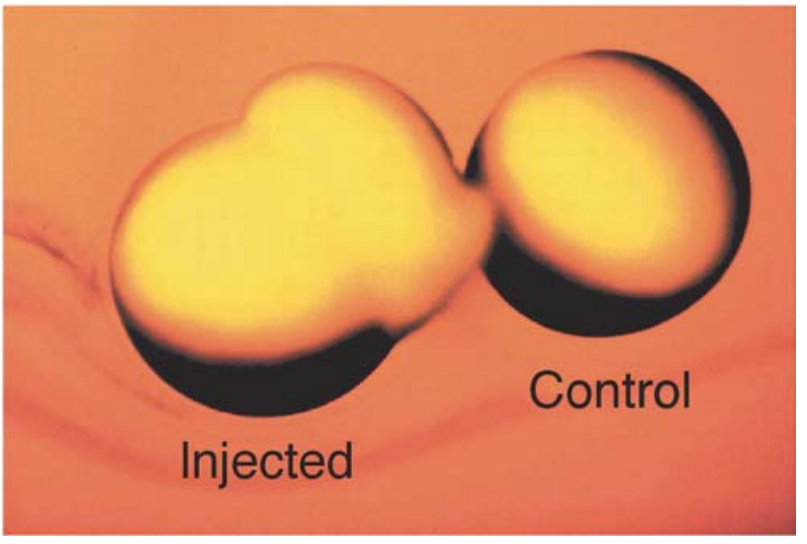

Fig. 1. The oocyte swelling assay demonstrating AQP1's water pore function. After transfer into hypotonic solution the oocyte expressing AQP1 (left) explodes due to massive water influx, whereas the control oocyte (right) does not experience a significant change in volume. (Figure adapted from Preston *et al.* 1992, reproduced with permission from *Science*.)

residue did not affect AQP1's water permeability, demonstrating that glycosylation is not important for AQP water conduction (Zhang *et al.* 1993a).

A non-functional mutant, Cys189Trp (Zhang *et al.* 1993a), was used to determine whether tetramerization was required for AQP1 to form a functional water pore. Chimeric cDNA dimers were constructed containing wild-type AQP1 in series with either wild-type or Cys189Trp mutant AQP1. Transcribed cRNAs were injected into oocytes, and plasma membrane expression was assayed. Immunofluorescence showed correct trafficking of the water pores to the plasma membrane and confirmed the formation of chimeric tetramers. Water conduction, measured by osmotic swelling, demonstrated that despite the obligatory assembly of AQP1 into tetramers, oligomerization was not required for the formation of functional water pores (Shi *et al.* 1994). This feature sets AQPs apart from ion channels, which usually have to oligomerize to form a channel in the center of the protein assembly. While none of the AQPs studied to date are stable in the membrane as a monomer, the reason why these proteins evolved to form tetramers remains unclear. Some AQPs display a marked propensity to form arrays. A tetramer featuring four identical sides constitutes a much better building block for the formation of a regular lattice than an asymmetric monomer. Tetramerization might thus be a prerequisite for array formation, which might be of biological relevance for some members of the AQP family, e.g. for AQP4 to function as osmosensor (Hiroaki *et al.* 2006).

2.2 Reconstitution of purified AQP1 into artificial lipid bilayers

In parallel to its functional characterization by expression in oocytes, AQP1 was also purified from red blood cells and reconstituted into artificial lipid bilayers (Zeidel *et al.* 1992). Reconstitutions at high lipid-to-protein ratios (LPRs) were used for functional characterizations, whereas reconstitutions at low LPRs were primarily aimed at growing two-dimensional (2D) crystals for electron crystallographic structure analysis.

Using high LPRs, AQP1 purified from red blood cell membranes was reconstituted into small unilamellar vesicles. These vesicles were loaded with carboxyfluorescein, and water efflux from the vesicles upon change from iso- to hyper-osmolar buffer solution was monitored as fluorescence quenching with a stopped-flow device (Zeidel *et al.* 1992). AQP1 proteoliposomes exhibited 50-fold higher water permeability than control liposomes, while no change in permeability to urea and protons was observed. The water permeability was reversibly inhibited by mercurials (Zeidel *et al.* 1992), and the coefficient of osmotic water permeability was similar in magnitude to that of intact red blood cell membranes (Zeidel *et al.* 1992, 1994).

When purified AQP1 was reconstituted at the low LPR of 1, large vesicles formed with a diameter of more than 2 μm that contained highly ordered crystalline arrays of AQP1 (Walz *et al.* 1994a). These 2D crystals were evaluated for water pore activity in the same way as the proteoliposomes. The AQP1 molecules in the vesicular 2D crystals exhibited the same high osmotic water permeability as those in the proteoliposomes, and water conduction could also be inhibited by incubation with $HgCl_2$. These results showed that the proteins in the 2D crystals were biologically active (Walz *et al.* 1994a). Water permeability was also measured over a range of temperatures revealing low Arrhenius activation energy of 1·9 kcal/mol, similar to diffusion of water in bulk solution.

2.3 Structural information deduced from the primary sequence

While structural studies were still in their infancy, much about the AQP1 structure could already be learned from the primary sequence. Hydropathy analysis predicted that AQP1 contains six membrane-spanning segments with five connecting loops (A–E) (Smith & Agre, 1991). Since AQP1 is glycosylated at Asn42 on loop A (Smith & Agre, 1991), this loop had to be extracellular, which localized both the N- and C-termini to the cytoplasm. This membrane topology was further confirmed by analysis of functional epitope-scanning mutants and vectorial proteolysis (Preston *et al.* 1994). Upon closer inspection of the sequence, it became evident that the N- and C-terminal halves of AQP1 were related and probably evolved by gene duplication (Pao *et al.* 1991). Since each tandem repeat only contains three transmembrane helices, the two repeats are oriented 180° to each other within the membrane, an arrangement that has meanwhile also been found in a number of other membrane pores, channels and transporters.

Each AQP1 repeat contains the highly conserved asparagine–proline–alanine (NPA) motif. The NPA motifs are located in the cytoplasmic loop B and the extracellular loop E. Since these two loops are rather hydrophobic in nature it was suspected that they were structural components of the aqueous pore. While the two loops are distant in the primary amino-acid sequence of AQP1, it was suggested that once the polypeptide chain was folded they would physically associate with each other within the membrane bilayer, giving rise to the hourglass model for the AQP pore architecture (Jung *et al.* 1994a).

2.4 Evolution and mammalian AQPs

The AQP family arose by tandem gene duplication (Pao *et al.* 1991). Since bacteria such as *E. coli* contain both a glycerol facilitator (GlpF) and a specific water pore (AQPZ), the gene duplication appears to have occurred early in evolution. The N-terminal segment has about 20% sequence conservation with the C-terminal segment (Wistow *et al.* 1991). To date, 13 mammalian AQPs have been reported (Fig. 2). Sequence identity among members of the AQP family ranges from

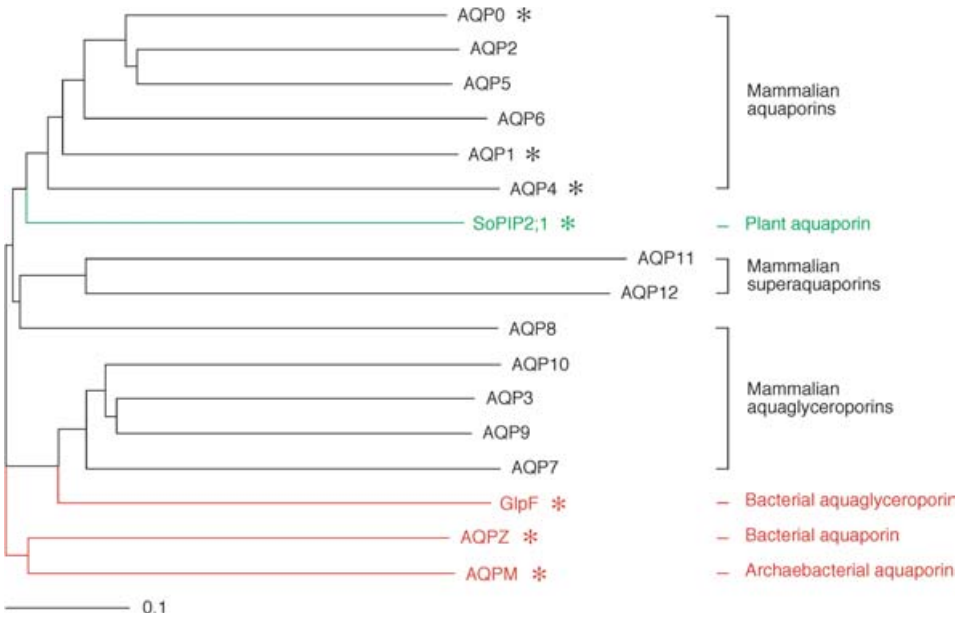

Fig. 2. Phylogenetic tree of mammalian AQPs and AQPs of known atomic structure. The sequences were aligned with T-Coffee (Notredame *et al.* 2000), and the tree was generated with the program TreeViewX, version 0.5.0.

about 25% to 40%. Based on the permeability properties of each pore, the AQP family is divided into two subfamilies, the aquaporins, which only allow water to permeate the pore, and the aquaglyceroporins, which are also permeable to glycerol and other small neutral solutes. Some archaeabacterial AQPs may form another subfamily that may lie in between the aquaporins and the aquaglyceroporins (see Section 3.7). AQPs 0, 1, 2, 4, 5, 6, and 8 are aquaporins, although AQP6 and AQP8 only belong to this group based on their sequence, since AQP6 forms an anion channel (Yasui *et al.* 1999a) and AQP8 has been reported to be permeable to urea (Ishibashi *et al.* 1997a; Ma *et al.* 1997). AQPs 3, 7, 9, and 10 are aquaglyceroporins, with AQP9 exhibiting the broadest substrate specificity (Tsukaguchi *et al.* 1998). The substrate specificities for the recently identified AQP11 and AQP12 (Ishibashi *et al.* 2000), named superaquaporins (Morishita *et al.* 2004), have not yet been determined. In the phylogenetic tree shown in Figure 2 we have also included the glycerol facilitator GlpF and the water pore AQPZ from *E. coli*, archaebacterial AQPM as well as plant SoPIP2;1, since these are additional AQPs with known atomic structures.

AQP0. The lens MIP was found in the mid-1970s and cloned in the early 1980s (Gorin *et al.* 1984). It is the major constituent of lens fiber cell membranes (Bloemendal *et al.* 1972), where it accounts for 60% of the total membrane protein content (Alcala *et al.* 1975). MIP was found to localize to membrane junctions (Bok *et al.* 1982), and proteoliposomes containing MIP tended to cluster and aggregate (Dunia *et al.* 1987). When reconstituted into planar lipid bilayers it appeared to form channels (Zampighi *et al.* 1985). MIP was thus initially thought to be a gap junction protein or a voltage-gated ion channel (Ehring *et al.* 1990), and it was suggested to have a dual role as an intercellular adhesion molecule and a volume-regulating channel (Zampighi *et al.* 1989). Its role as a water pore was only established once AQP1 was identified as a water pore, and it is now referred to as AQP0. Expression of AQP0 in oocytes increases water permeability by a factor of 4–5 (Mulders *et al.* 1995). Its water pore activity is thus much lower than that of AQP1

(Chandy *et al.* 1997) and other AQPs. AQP0 was also found to increase oocyte glycerol permeability by a factor of about 3 (Kushmerick *et al.* 1995), but this function was not found in lens fiber cells (Varadaraj *et al.* 1999). Mutations in AQP0 result in defects of lens development and cataracts (reviewed in Chepelinsky, 2003).

AQP2. Homology cloning was used to isolate the cDNA encoding AQP2 from the renal collecting duct (Fushimi *et al.* 1993). Expression of the protein in oocytes showed the pore to be permeable to water in a mercury-sensitive way (Zhang *et al.* 1993b). AQP2 is regulated by vasopressin (Zhang *et al.* 1993b), which causes the protein to shuttle from intracellular stores to the membranes of the collecting duct epithelium (Nielsen *et al.* 1995). Defective AQP2 trafficking causes nephrogenic diabetes insipidus, a condition characterized by the kidney's inability to produce concentrated urine because of the insensitivity of the distal nephron to vasopressin (reviewed in Nguyen *et al.* 2003).

AQPs 4, 5, 6, and 8. AQP4 is the predominant water pore in brain (Hasegawa *et al.* 1994; Jung *et al.* 1994b) and is highly expressed in glial membranes that are in direct contact with capillaries (Nielsen *et al.* 1997a). AQP4 null mice resist brain swelling following cytotoxic edema produced by acute water intoxication and ischemic stroke (reviewed in Verkman, 2005), indicating that AQP4 may be important in regulation of water balance in the brain (Jung *et al.* 1994b; Nielsen *et al.* 1997a). Two cDNAs for AQP4 were isolated corresponding to two initiating methionines, M1 and M23 (Lu *et al.* 1996). Expression of either splicing variant in oocytes increased osmotic water permeability 20-fold, which was not affected by $HgCl_2$ (Jung *et al.* 1994b). AQP5 was isolated from salivary gland cDNA (Raina *et al.* 1995). It resides at the apical membranes of type 1 alveolar pneumocytes as well as in a subset of salivary and lachrymal glands, where it presumably regulates airway humidification and the release of saliva and tears (Nielsen *et al.* 1997b). AQP6, another AQP expressed in the kidney, is localized mostly in intracellular vesicles (Yasui *et al.* 1999b). Its water conduction is poor but it is also permeable to anions, with permeability for halides following the sequence $NO_3^- > I^- \gg Br^- > Cl^- \gg F^-$ (Yasui *et al.* 1999a; Ikeda *et al.* 2002). Asn60 has been shown to be involved in anion selectivity, and substitution of this residue to glycine abolished anion permeability, resulting in a pore that was only permeable to water (Liu *et al.* 2005). AQP8 is expressed in hepatocytes (Calamita *et al.* 2001) and may be permeated by water and urea (Ishibashi *et al.* 1997b; Ma *et al.* 1997). Like AQP6, it is primarily expressed in an intracellular location. It redistributes to the canalicular membrane upon stimulation with the hormone glucagon, a process that involves cAMP/protein kinase A (Gradilone *et al.* 2003, 2005).

AQPs 3, 7, 9, and 10. The aquaglyceroporin family includes AQP3 that functions as a glycerol facilitator in the skin (Hara-Chikuma & Verkman, 2005) and AQP7 whose principle site of expression is the plasma membrane of adipocytes (Ishibashi *et al.* 1997a). AQP7 null mice attain a much greater fat mass than wild-type mice as they age (reviewed in Verkman, 2005). AQP9 was cloned from liver, where it confers high permeability for both water and solutes (Ishibashi *et al.* 1998). AQP9 is insensitive to mercury and mediates passage of a wide variety of non-charged solutes including urea, polyols (e.g. glycerol and mannitol), purines and pyrimidines (Tsukaguchi *et al.* 1998). AQPs 7 and 9 are closely related and are the only aquaglyceroporins known to be permeated by arsenite (Liu *et al.* 2002). AQP10 was cloned from the small intestine (Ishibashi *et al.* 2002). When expressed in *Xenopus* oocytes AQP10 increased glycerol and urea uptakes as well as osmotic water permeability by a factor of 6 and was inhibited by $HgCl_2$ (Ishibashi *et al.* 2002).

AQPs 11 and 12. The most recently identified AQPs: AQP11 and AQP12 (Ishibashi *et al.* 2000), are unusual in that only the NPA motif in loop E is conserved, whereas the NPA motifs in

Table 1. *Mammalian aquaporins and aquaporins with known atomic structure*

Protein	Swiss-PROT ID	PDB ID	Regulation
AQP0	P30301	1SOR, 1YMG, 2B6O, 2B6P	pH, calcium/calmodulin
AQP1	P29972	1FQY, 1H6I, 1J4N	Phosphorylation
AQP2	P41181	–	Vasopressin, phosphorylation
AQP3	Q92482	–	pH
AQP4	P55087	2D57	Phosphorylation
AQP5	P55064	–	Phosphorylation
AQP6	Q13520	–	pH
AQP7	O14520	–	
AQP8	O94778	–	Glucagon
AQP9	O43315	–	Estrogen
AQP10	Q96PS8	–	
AQP11	Q8NBQ7	–	
AQP12	Q8IXF9	–	
AQPZ	P60844	1RC2, 2ABM	
GlpF	P11244	1LDA, 1LDI, 1LDF	
AQPM	Q9C4Z5	2EVU, 2F2B	
SoPIP2;1	P43286	1Z98, 2B5F	pH, phosphorylation

loop B are NPC and NPT, respectively. Expression of these two AQPs in *Xenopus* oocytes has proved difficult, and their substrate specificity has therefore not yet been established.

AQPs vary in their water permeability, with AQP0 being the least efficient and AQP1 and AQP4 being the most efficient water pores (Yang & Verkman, 1997). The diversity and large number of AQPs in the genome reflects the strict control of permeation through these pores, required for diverse functions of cells and organs for the regulation of water homeostasis (reviewed in Agre & Kozono, 2003; King *et al.* 2004). The function of individual AQP homologs was reviewed in Lee *et al.* (1998). For a review and listing of immunohistochemical localization of mammalian AQPs see Matsuzaki *et al.* (2002). (For reviews concerned with molecular mechanisms for human diseases see Borgnia *et al.* 1999; Agre *et al.* 2001; Agre & Kozono, 2003). This review concentrates on the structure of AQPs. A summary of AQPs of known atomic structures with their protein data bank and Swiss-Prot accession numbers together with regulatory elements is presented in Table 1.

3. Chronological overview of AQP structures

Since their discovery, AQPs have proved to be amenable to structural studies by both electron crystallography of 2D crystals and X-ray crystallography of 3D crystals. The AQP family has thus become one of the structurally best-characterized families of membrane proteins, and much has been learned on the structural basis of their function as membrane pores.

3.1 AQP1 – the red blood cell water pore

Studies on the AQP structure began with electron crystallographic analyses of 2D crystals of AQP1 purified from red blood cells. Two projection maps (Mitra *et al.* 1994; Walz *et al.* 1994a) and a 3D reconstruction (Walz *et al.* 1994b) produced with negatively stained AQP1 crystals confirmed the tetrameric organization of AQPs, and stopped-flow measurements showed that

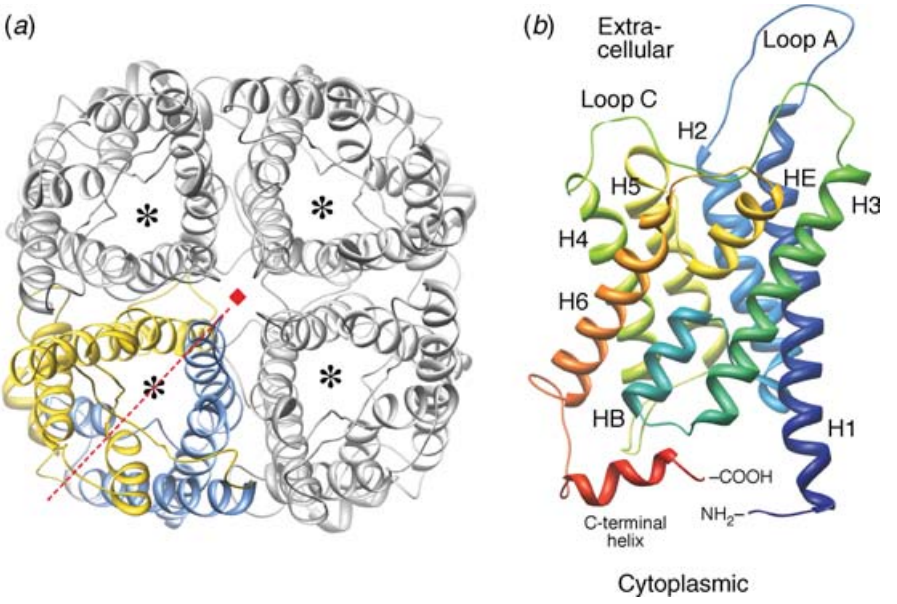

Fig. 3. Atomic model of AQP1. (*a*) AQP1 tetramer viewed from the extracellular surface. One monomer is colored in blue representing the N-terminal and yellow the C-terminal tandem repeat. The red dashed line indicates the pseudo-2-fold axis relating the two halves of the monomer, and the red square indicates the 4-fold axis of the tetramer. The asterisks indicate the water pore in each of the four subunits. (*b*) AQP1 monomer viewed in the direction parallel to the membrane. Membrane-spanning helices are denoted as H1–H6, loops are denoted as A–E, and the two pore helices formed by loops B and E as HB and HE, respectively.

the proteins in the crystalline arrays were biologically active (Walz *et al.* 1994a). Significant improvement in resolution was achieved once AQP1 2D crystals were visualized by cryo-electron microscopy, which initially produced projection maps (Jap & Li, 1995; Mitra *et al.* 1995; Walz *et al.* 1995) and then 3D density maps that revealed the organization of the six trans-membrane α-helices (Cheng *et al.* 1997; Li *et al.* 1997; Walz *et al.* 1997). The density maps showed that the helices in AQP1 form a right-handed bundle enclosing a vestibule that was believed to contain the water-selective pore and the functionally important NPA-carrying loops B and E (Cheng *et al.* 1997; Walz *et al.* 1997). A density map at the improved resolution of 4·5 Å later confirmed the location of loops B and E in the middle of the monomer (Mitsuoka *et al.* 1999).

In 2000, electron crystallographic analyses reached a resolution of 3·8 Å. The use of a very stable electron microscope with a helium-cooled, top-entry specimen stage (Fujiyoshi, 1998) was essential to record the many high-resolution images that were needed to produce a density map at this resolution. The final density map was sufficient to build an atomic model for AQP1, revealing for the first time the architecture of an AQP water pore (Murata *et al.* 2000) (Fig. 3). The atomic model confirmed the pseudo-2-fold symmetry of the protein. When starting from the 4-fold axis of the tetramer the helices in the two repeats are arranged as 2–1–3 (first repeat) and 5–4–6 (second repeat). The first repeat begins with the cytoplasmic N-terminus, followed by transmembrane helices 1 and 2 that are connected on the extracellular side by extended loop A, which contains the glycosylation site Asn42 (Smith & Agre, 1991). Loop B connecting trans-membrane helices 2 and 3 folds back into the membrane and places the first NPA motif midway through the membrane. Immediately after the NPA motif, loop B reverses its direction and

forms a short helix, named pore helix HB, which brings the polypeptide chain back to the cytoplasmic side of the membrane. Transmembrane helix 3 concludes the first repeat of AQP1. The first and second repeats are connected by loop C that spans the entire extracellular surface of the monomer. The second repeat is oriented 180° to the first repeat and begins at the extracellular surface. Transmembrane helices 4 and 5 are connected by cytoplasmic loop D. Like loop B in the first repeat, loop E connecting helices 5 and 6 again folds back into the membrane, placing the second NPA motif opposite the first NPA motif in the middle of the bilayer. The two NPA motifs are held together in the center of the monomer by van der Waals interactions between the proline residues of the two NPA motifs. Immediately following the second NPA, loop E forms another short helix, pore helix HE, that brings the chain back to the extracellular side of the membrane. Helix 6 is the last membrane-spanning segment, emerging on the cytoplasmic side, where the AQP1 molecule ends (Murata *et al.* 2000). This novel fold was later confirmed by an X-ray structure of AQP1 at 2·2 Å resolution, which also revealed a short α-helix in the C-terminus of AQP1 (Sui *et al.* 2001). This fold was found to be conserved in all AQP structures determined to date.

AQP1 tetramers are held together by extensive interactions between the monomers. Transmembrane helices 1 and 2 from one monomer form a left-handed coiled-coil interaction with helices 4 and 5 of a neighboring monomer. Helices from neighboring monomers also interact outside the membrane: helix 1 interacts with helix 5 of the adjacent monomer at the extracellular surface and helix 2 interacts with helix 4 of the adjacent monomer at the cytoplasmic surface. Interactions between loops may also contribute to tetramer stability with loop A of the four monomers surrounding the 4-fold axis of the tetramer on the extracellular surface (Murata *et al.* 2000; Sui *et al.* 2001).

Pore helices HB and HE contain highly conserved residues that line one surface of the AQP1 water pore. Residues originating from helices 2 and 5 and the C-terminal halves of helices 1 and 4 form the remaining surface of the pore. Six water molecules were found to form a single file through the pore of AQP1 (Sui *et al.* 2001). These water molecules form hydrogen bonds with side-chain carbonyls from six residues in helices HB and HE, which are Gly74, Ala75, His76 (on the cytoplasmic side) and the pseudo-2-fold symmetry-related residues Gly190, Cys191 and Gly192 (on the extracellular side) (Sui *et al.* 2001). The EM structure revealed that the physical limitation on the size of substrates allowed to permeate the AQP1 pore is imposed by a narrowing of the pore to a diameter of 3 Å (Murata *et al.* 2000), which is only slightly larger than the 2·8 Å diameter of a water molecule. In addition, unlike ion channels, such as the KcsA potassium channel (Doyle *et al.* 1998), AQP1 does not contain a structure to liberate ions from their hydration shell. The pore constriction therefore prevents permeation of all molecules bigger than water, including hydrated ions. This finding is consistent with biophysical measurements that showed that AQP1 is impermeable to solutes and ions (Zeidel *et al.* 1992, 1994). The narrow pore region was also seen in the X-ray structures of GlpF, where it was called the selectivity filter (Fu *et al.* 2000), and AQP1, where it was named the ar/R constriction site, because it contains a highly conserved aromatic and arginine residues (Sui *et al.* 2001). The ar/R constriction site in AQP1 is formed by Arg197, His182, Phe58 and Cys189 (Sui *et al.* 2001). Cys189 is the site for blockage of AQP1 by $HgCl_2$ (Preston *et al.* 1993; Zhang *et al.* 1993a). Its side-chain extends into the pore from the extracellular side of the constriction site indicating that inhibition by $HgCl_2$ is a result of physical blocking of the aqueous pathway (Murata *et al.* 2000). Arg197 and His182 line one side of the pore creating a hydrophilic surface while Phe58 is located on the opposite side.

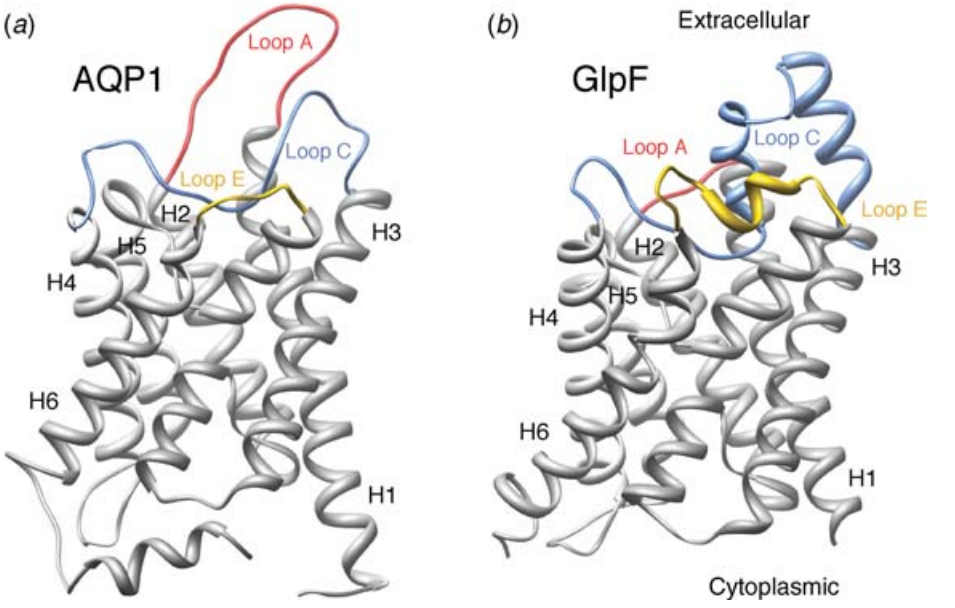

Fig. 4. Comparison of the AQP1 and GlpF structures. (*a*) AQP1; (*b*) GlpF. The main differences in the fold are the conformations of extracellular loops A (red), C (blue), and E (yellow). The helix-turn-helix motif formed by loop C in GlpF may function as a funnel for the pore.

3.2 GlpF – the *E. coli* glycerol facilitator

GlpF is the glycerol facilitator in *E. coli*. Its permeability to glycerol, urea and glycine was established by 1980 (Heller *et al.* 1980), but GlpF was not recognized as a member of the AQP family until the early 1990s (reviewed in Agre *et al.* 1993), probably because its water permeability is much lower than that of water-specific AQPs (Maurel *et al.* 1994). The structure of GlpF was determined to 2·2 Å resolution by X-ray crystallography (Fu *et al.* 2000; reviewed in Nollert *et al.* 2001) shortly after the AQP1 structure was solved (Murata *et al.* 2000). The crystal structure showed the same right-handed bundle of six α-helices seen in AQP1 (Murata *et al.* 2000; Ren *et al.* 2001; Sui *et al.* 2001), but also revealed three glycerol molecules (G1–G3) in the pore. Two years later a crystal structure for GlpF in the absence of glycerol molecules was published, which showed nine water molecules in the pore (Tajkhorshid *et al.* 2002). The two GlpF structures are virtually identical, with some minor differences in the positions of amino-acid side-chains along the pore, which helped our understanding of the specificity of this pore and how it selects for certain sugars while not accommodating others (reviewed in Stroud *et al.* 2003a, b; see Section 5).

The GlpF structure (Fu *et al.* 2000; Tajkhorshid *et al.* 2002) showed that this aquaglyceroporin adopts essentially the same fold seen in the water pore AQP1 (Murata *et al.* 2000; Ren *et al.* 2001; Sui *et al.* 2001) with six membrane-spanning helices and two half helices forming a right-handed bundle surrounding an aqueous pore. The main differences in the structures of AQP1 and GlpF are found in the extracellular loops (Fig. 4). Loop A is much shorter in GlpF than in AQP1. Loop C, which connects the two tandem repeats, lies flat on the extracellular surface in AQP1, but is extended in GlpF and forms a helix-turn-helix motif. The function of this helix-turn-helix motif

is not yet understood but has been proposed to function as a funnel for the pore (Fu *et al.* 2000). Loop E, the NPA-carrying loop in the second tandem repeat, is longer in GlpF than in AQP1 and forms a one-turn helix before connecting with transmembrane helix 6.

To allow larger substrates such as glycerol to permeate, the constriction site in the GlpF pore has to be larger and more hydrophobic than that in the pore of AQP1. This is accomplished by a number of substitutions in residues forming the constriction site of GlpF. His182 of AQP1 is replaced by a much smaller glycine residue (Gly191). This allows room for two additional substitutions: Cys191 of AQP1 is replaced by the much more hydrophobic Phe200 and Phe58 of AQP1 by the larger Trp48. Arg206 of GlpF is equivalent to Arg197 of AQP1 (Fu *et al.* 2000; Sui *et al.* 2001). The absence of a cystein at the constrictions site in GlpF explains why its conduction is not sensitive to mercurials. The resulting constriction site has a larger diameter of 3·8 Å, which is large enough to accommodate a glycerol molecule (Fu *et al.* 2000) (see Section 5). The polar side of the amphipatic pore is formed by six hydrogen bond acceptors lining up in the GlpF pore from top to bottom: the carbonyls of Phe200, Ala201 and Gly199 on the periplasmic side, and the pseudo-2-fold related carbonyls of His66, Ala65 and Gly64 in the cytoplasmic vestibule.

3.3 AQPZ – the *E. coli* water pore

The *E. coli* water pore AQPZ shares a high amino-acid sequence similarity with the *E. coli* glycerol facilitator GlpF. The two proteins vary, however, greatly in their water permeability, with GlpF conducting water at a rate that is only about one sixth that of AQPZ (Borgnia & Agre, 2001).

The structure of AQPZ was determined by X-ray crystallography to 2·5 Å resolution (Savage *et al.* 2003). The AQPZ tetramers crystallized in a *p*4 space group with two protomers (A and B) per asymmetric unit. AQPZ adopts the cannonical AQP fold. The pore itself is lined by residues originating from helices M1–M3 (H1, H2 and HB in AQP1) and the pseudo-2-fold related M5–M7 (H4, H5 and HE in AQP1). The constriction site of AQPZ is formed by the side-chains of Arg189, Phe43, His174 and Thr183, narrowing the pore to a diameter of 2 Å (Savage *et al.* 2003). On the N-terminal half of the pore, the hydrophilic face consists of four adjacent carbonyls of Gly59, Gly60, His61 and Phe62, while on the C-terminal pseudo-2-fold related half of the pore the four carbonyls are contributed by Asn182, Tyr183, Ser184 and Val185. The hydrophobic face of the pore results from an abundance of valines, phenylalanines and isoleucines within the pore. The pore is narrow at the center of the membrane but widens out above and below to form the periplasmic and cytoplasmic vestibules in a similar fashion to other AQPs.

The water pore structure differed between the two AQPZ protomers in the asymmetric unit (Savage *et al.* 2003). Protomer A contained a continuous line of five hydrogen-bonded water molecules in its pore. In contrast, protomer B contained only three water molecules, and during molecular dynamic simulations these waters left the pore (Wang *et al.* 2005). The main difference in the pore lining residues between protomers A and B is the position of Arg189 of the AQPZ constriction site (Savage *et al.* 2003), which adopts different conformations in the two protomers (Wang *et al.* 2005) (Fig. 5). In the water-filled pore of protomer A, Arg189 is in an 'UP' position, which is the conformation seen in most AQP crystal structures. In protomer B, which contains only three water molecules, Arg189 is in the 'DOWN' position, which was only seen in AQP0 (see below). In a more recent crystal structure of AQPZ, Arg189 was seen to adopt the two different conformations in different subunits of the same tetramer (Jiang *et al.* 2006).

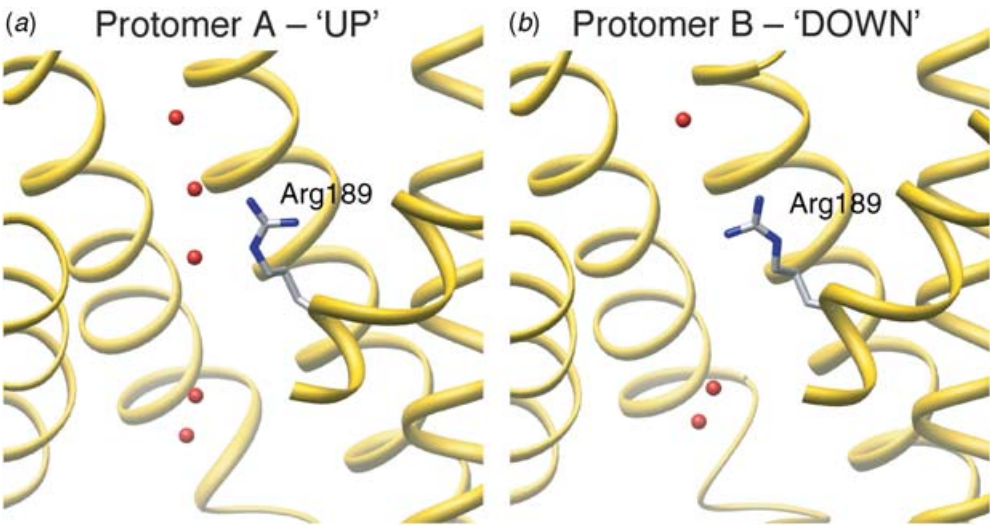

Fig. 5. The two conformations of Arg189 in AQPZ. (*a*) The 'UP' state has been seen in most AQP structures determined to date. (*b*) The 'DOWN' state has so far only been seen in X-ray structures of AQPZ and the EM structure of AQP0.

3.4 AQP0 – the lens-specific aquaporin

AQP0 is only expressed in the fiber cells of the eye lens, where it is the major membrane protein (Bloemendal *et al.* 1972; Alcala *et al.* 1975). AQP0 is permeable to glycerol *in vitro* (Kushmerick *et al.* 1995), but only water conduction was observed *in vivo* (Varadaraj *et al.* 1999). The permeability of AQP0 for water is about 40 times lower than that of AQP1 (Chandy *et al.* 1997), but it can double under mildly acidic conditions (Nemeth-Cahalan & Hall, 2000; Varadaraj *et al.* 2005), such as those found in the core of the lens (Mathias *et al.* 1991). AQP0 also forms the 11–13 nm thick 'thin junctions' between lens fiber cells (Costello *et al.* 1989), which consist of square AQP0 arrays. The adhesive properties of AQP0 have also been demonstrated *in vitro* in a number of ways, including clustering of AQP0 proteoliposomes (Dunia *et al.* 1987) and electron and atomic force microscopy of reconstituted AQP0 2D crystals that turned out to be double-layered (Hasler *et al.* 1998; Fotiadis *et al.* 2000). Furthermore, AQP0 exists as a full-length protein of 26 kDa in young lens fiber cells, but upon ageing it undergoes proteolysis to a 22-kDa form (Roy *et al.* 1979; Takemoto *et al.* 1986; Zampighi *et al.* 1989). This cleavage has been shown to induce junction formation (Kistler & Bullivant, 1980; Gonen *et al.* 2004b), while it does not seem to affect the permeability properties of AQP0 (Ball *et al.* 2003).

Reconstitution of protein purified from the lens core, where AQP0 exists as a mixture of full-length and truncated protein, into artificial lipid bilayers produced large double-layered 2D crystals, which were used to determine the structure of AQP0 by electron crystallography to 3 Å resolution (Gonen *et al.* 2004a). The crystals with *p*422 symmetry had lattice dimensions of $a = b = 65{\cdot}5$ Å and a thickness of 11 nm, reproducing the exact dimensions of the thin junctions between lens fiber cells (Costello *et al.* 1989; Zampighi *et al.* 1989). AQP0 shares the same fold as all other AQPs, but has unique features that enable it to form membrane junctions (Gonen *et al.* 2004a). In the crystals two apposing tetramers interact with each other via their extracellular

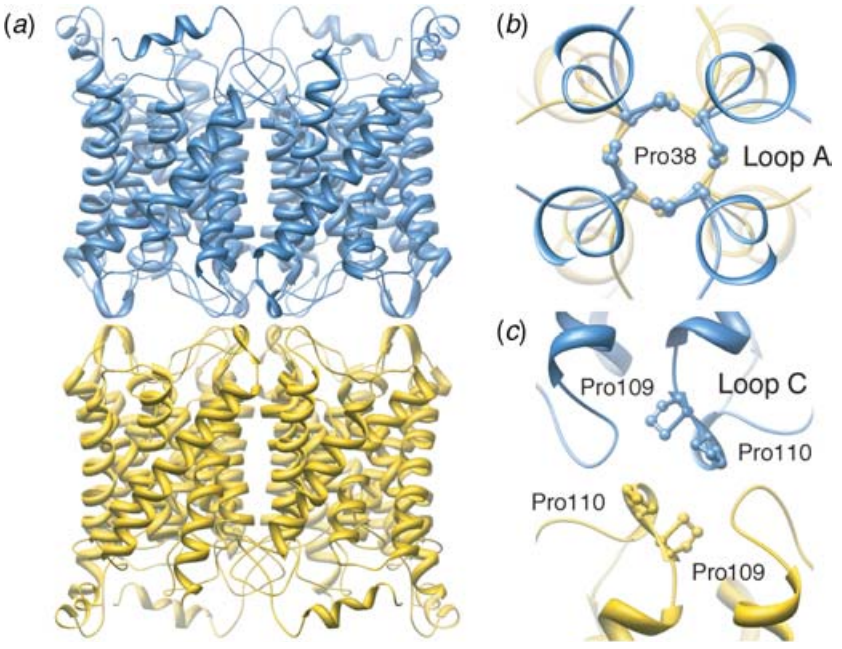

Fig. 6. Membrane junction formed by truncated AQP0. (*a*) Two interacting AQP0 tetramers (colored in blue and yellow) viewed in the direction parallel to the membranes. (*b*) Pro38 in loop A of all eight subunits in the stacked tetramers form a rosette-like structure that stabilizes the membrane junction through proline–proline stacking interactions. (*c*) A di-proline motif formed by Pro109 and Pro110 in loop C is also involved in junction formation through proline–proline stacking interactions with the di-proline motif in the symmetry-related subunit of the apposing tetramer.

domains. Junction-forming interactions in AQP0 are facilitated by small extracellular loops and the lack of glycosylation. The resulting flat extracellular surface allows two opposing AQP0 tetramers to approach each other and to make specific contacts mediated by the corresponding loops in the opposing AQP0 molecules. The interactions are mainly mediated by proline residues, which are conserved in AQP0s from different species but substituted in other AQPs (Fig. 6). The Pro38 residue in loop A from all eight subunits come together at the center of two interacting tetramers and form a rosette-like structure. Loop C, connecting the two tandem repeats, contains proline residues 109 and 110, which pack against symmetry-related prolines 109 and 110 from the opposing tetramer (Gonen *et al.* 2004a, 2005).

The water pore in the structure of junctional AQP0 appeared to be in a closed conformation (see Section 6). Unlike AQP1, GlpF and AQPZ, AQP0 contains two constrictions sites, one in each vestibule (Gonen *et al.* 2004a). The first constriction site, CS-I, is equivalent to the ar/R constriction site described for AQP1 (Sui *et al.* 2001), which is formed in AQP0 by Arg187, Phe48, Ala181 and His172. AQP1's Cys191 is substituted in AQP0 by Ala181, explaining why AQP0 permeability is insensitive to mercury (Varadaraj *et al.* 1999). The fact that AQP0 contains His172 at its constriction site, a residue that is only found in specific water pores and is substituted in glycerol facilitators (Fu *et al.* 2000; Sui *et al.* 2001; Tajkhorshid *et al.* 2002), agrees with experimental results that show that AQP0 is not permeable to glycerol *in vivo* (Varadaraj *et al.* 1999). AQP0 contains a second, novel constriction site, CS-II, which is formed by Tyr149, His66 and Phe75 close to the cytoplasmic entrance of the pore (Fig. 7*a*). Tyr149 displays a relatively

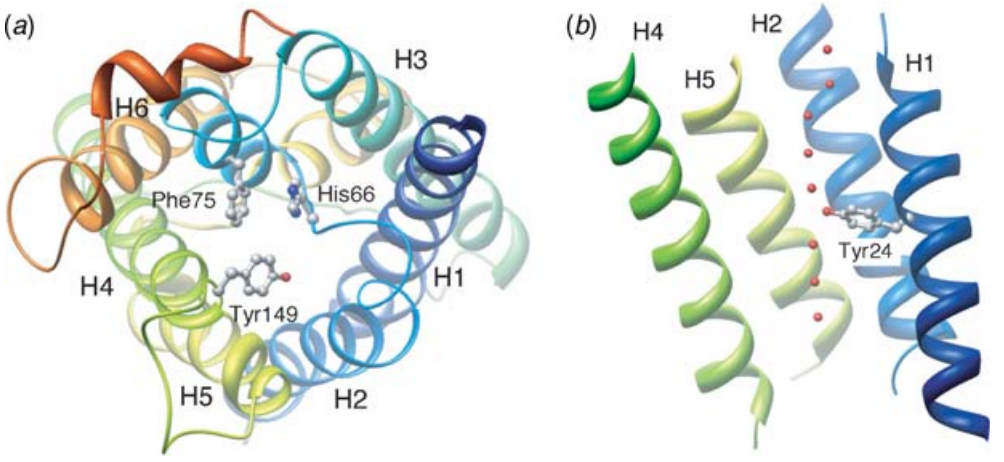

Fig. 7. Structural features of the AQP0 pore. (*a*) Residues His66, Phe75 and Tyr149 form a second constriction site close to extracellular pore opening. This might constitute the mechanism for pH regulation of AQP0 with His66 being the pH sensor and Tyr149 forming the flap. (*b*) The hydroxyl group of Tyr24 (here seen in the open pore) extends into the water pathway. The conformation of this residue may be responsible for the low water conduction rate of AQP0.

high B factor, indicative of high side chain mobility. Its hydroxyl group is also not hydrogen-bonded and the side-chain has sufficient space to change its conformation. These structural features suggest that Tyr149 could swing out to open the water pore, constituting a possible gating mechanism (Gonen *et al.* 2004a). Another unusual feature of the AQP0 pore is Tyr24, whose side-chain extends into the water pathway. While in other AQPs the water molecules in the pore form a continuous hydrogen-bonded line, the side-chain of Tyr24 in AQP0 coordinates water molecules and disrupts the continuity of the hydrogen bonding between water molecules in the pore. Tyr24 thus creates a 'phenolic barrier' (Fig. 7*b*) which may be responsible for the poor water conductance of AQP0 as compared to other AQPs (Gonen *et al.* 2005).

Shortly after the 3 Å EM structure of junctional AQP0 was published, the structure of full-length, non-juncional AQP0 was determined by X-ray crystallography to 2·2 Å resolution (Harries *et al.* 2004). The structure was almost identical to that of junctional AQP0, except that the water pore contained seven water molecules. This is in agreement with the notion that non-junctional AQP0 is predominantly in the open pore conformation, whereas junction formation stabilizes the water pore in the closed conformation. Recently, the resolution of the EM structure of junctional AQP0 was improved to 1·9 Å (Gonen *et al.* 2005). The density map at this resolution revealed only three water molecules in the pore that were too far apart to form hydrogen bonds, thus confirming that the water pore in junctional AQP0 is indeed in a closed conformation (for a discussion of the mechanism see Section 6.4).

Comparison between the structures of full-length, non-junctional AQP0 and truncated, junctional AQP0 provides a possible hint as how cleavage of AQP0's cytoplasmic N- and C-termini may result in junction formation on the extracellular side of the protein. Residues in the N- and C-termini of full-length AQP0 engage in a number of specific interactions. The C-terminus is stabilized by electrostatic interactions formed by C-terminal residues Arg226 and Lys228 with residues Ser79, Gln80 and Asp150. The N-terminus loops back and tucks Trp2 into a hydrophobic pocket formed by residues Phe9, Trp10 and Leu84 from helices 1 and 2. The resulting

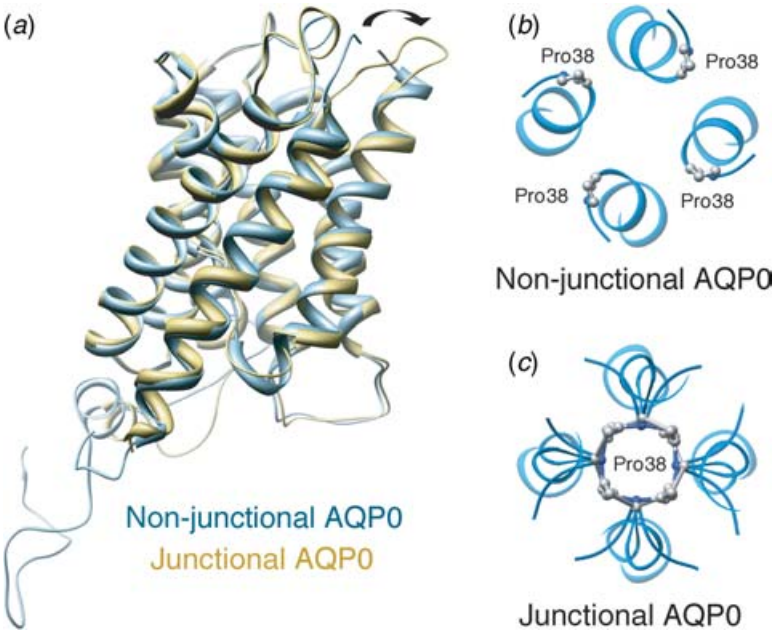

Fig. 8. Conformational change in AQP0 upon junction formation. (*a*) Overlay of the X-ray structure of non-junctional (blue) and the EM structure of junctional AQP0 (yellow). The arrow indicates the movement of extracellular loop A potentially elicited by the truncation of the cytoplasmic termini, allowing the AQP0 tetramers to form a junction. (*b*) In non-junctional AQP0, loop A adopts a conformation, in which Pro38 is in a position that is not conducive to the stabilization of a membrane junction. (*c*) After the conformational change in loop A, Pro38 is in a position, in which it can form the junction-stabilizing rosette-like structure.

conformation of the N-terminus allows Glu3 to interact with Ser240, an interaction that forms a bridge between N- and C-terminus. These interactions are eliminated in truncated AQP0, which may be the cause for the conformational change in loop A on the extracellular side of the membrane, which brings Pro38 into a position where it can engage in junction-forming interactions (Gonen *et al.* 2005) (Fig. 8). Recently another X-ray crystal structure of AQP0 at 7 Å resolution was published showing paired AQP0 tetramers (Palanivelu *et al.* 2006). The interactions between the extracellular surfaces of the detergent-solubilized AQP0 tetramers are different from those observed in the 2D crystals. The main difference is that Pro123, rather than Pro110 as in the EM structure, inserts into the pocket formed by Pro109, Ala111 and Pro123. While the nature of the interaction remains the same, the insertion of Pro123 into the binding pocket results in a 24° rotation of the two teramers with respect to each other. This interaction can therefore only occur between isolated tetramers but not between AQP0 arrays.

A unique feature of the 1·9 Å electron crystallographic density map of junctional AQP0 is that it revealed a continuous lipid bilayer surrounding the AQP0 tetramers (Gonen *et al.* 2005). The lipids are often sandwiched between two AQP0 tetramers and mediate the crystal contacts in the 2D arrays. Since the lipids did not co-purify with the protein, the interactions of AQP0 with its surrounding lipids must be non-specific in nature. Of the nine visualized lipid molecules, seven lipids (PC1–PC7) are in direct contact with the protein and are thus 'annular lipids', whereas two lipids (PC8 and PC9) are not in contact with protein and represent 'bulk lipids' (Fig. 9). Since the unit cell dimensions of the AQP0 2D crystals are the same as those in thin junctions between lens fiber cells (Zampighi *et al.* 1982), the observed lipid–protein interactions are likely to be

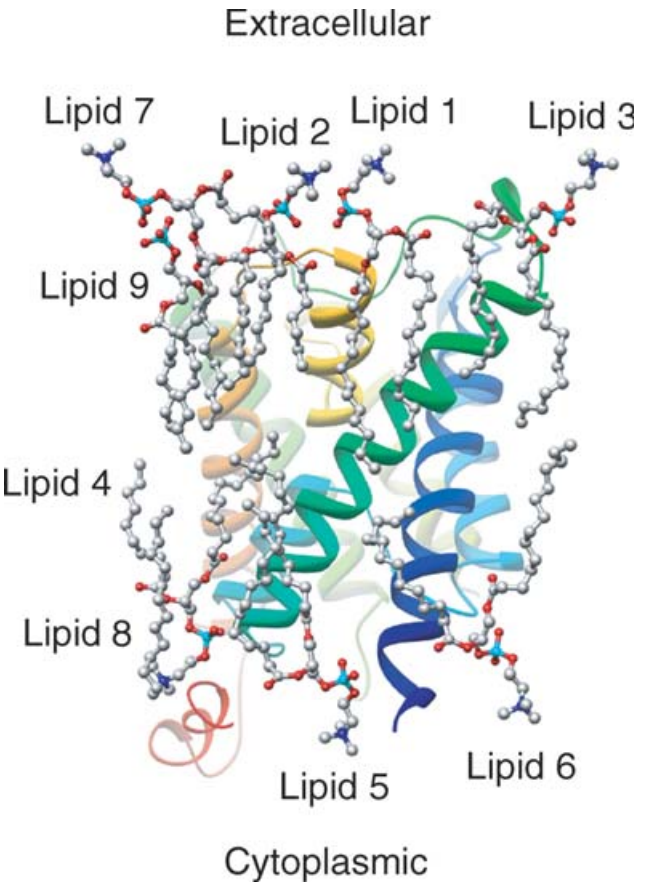

Fig. 9. Lipids visualized in the EM structure of junctional AQP0. Each AQP0 monomer is surrounded by nine lipids. Lipids 1–7 are annular lipids that are in direct contact with the protein, whereas lipids 8 and 9 have no contact with protein and represent bulk lipids.

representative of those formed by AQP0 tetramers with native lipids in lens fiber cell membranes (Gonen *et al.* 2005).

3.5 AQP4 – the main aquaporin in brain

AQP4 is the predominant water pore in brain (Hasegawa *et al.* 1994; Jung *et al.* 1994b), where it localizes to glial cells. Its water conductance is insensitive to $HgCl_2$ (Jung *et al.* 1994b) and it forms orthogonal arrays *in vivo* (Rash *et al.* 1998). AQP4 exists in two isoforms, starting with Met1 (AQP4M1) and Met23 (AQP4M23), respectively (Lu *et al.* 1996).

The protein used to determine the structure of AQP4 was produced in insect cells, making AQP4 the first mammalian AQP whose structure was obtained with recombinant protein (Hiroaki *et al.* 2006). When AQP4M23 was reconstituted into artificial lipid bilayers, it formed double-layered 2D crystals (Hiroaki *et al.* 2006). Electron crystallographic structure analysis revealed that AQP4 tetramers in the two membranes interact through their extracellular surfaces. Unlike in double-layered 2D crystals of AQP0, AQP4 tetramers in the two crystalline layers are shifted relative to each other by half a unit cell, establishing a $p42_12$ symmetry. Each AQP4

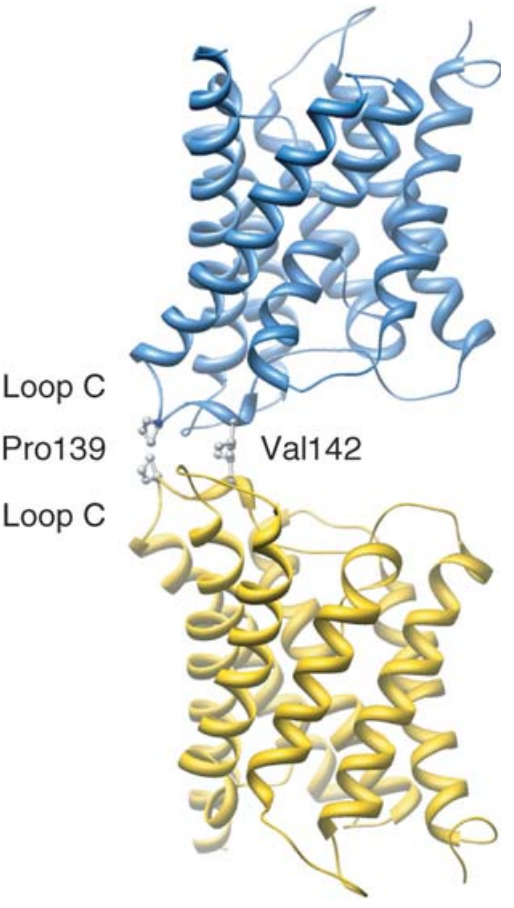

Fig. 10. Membrane junction formed by AQP4. The two interacting AQP4 monomers (colored in blue and yellow) are viewed in the direction parallel to the membranes. Junction formation is mediated by residues Pro139 and Val142, which are part of short helix HC in extracellular loop C.

tetramer thus interacts with four tetramers in the adjoining membrane. The AQP4 molecule adopts the canonical AQP fold, but features an additional short 3_{10} helix in extracellular loop C, helix HC, formed by residues Ser140 to Gly143 (Fig. 10). Two residues in helix HC, Pro139 and Val142, mediate the interactions between apposing AQP4 tetramers, which are specific but much weaker than the junction-forming interactions seen in AQP0. Because the interactions between AQP4 tetramers in adjoining membranes are weak, the distance and relative orientation of the two membranes in the double-layered 2D crystals varied, which made structure determination exceptionally difficult. Despite the weakness of the interactions between AQP4 tetramers, expression of AQP4M23 in L cells induced the cells to cluster (Hiroaki *et al.* 2006). Furthermore, immunolabeling of thin sections through the hypothalamus localized AQP4 to junctional as well as non-junctional membrane areas, suggesting that junction formation is a physiologically relevant function of AQP4 (Hiroaki *et al.* 2006).

The AQP4 structure also revealed the reason why only AQP4M23, but not AQP4M1, can form orthogonal lattices. It was initially thought that the bulk of the additional N-terminal 22 amino acids would prevent AQP4M1 from array formation (Furman *et al.* 2003). The structural

studies on the AQP4 arrays suggest, however, that destabilization of crystalline arrays is not merely due to sterical hinderance because of the bulkiness of the N-terminus, but that it is a specific characteristic of the amino-acid sequence of the native N-terminus (Hiroaki *et al.* 2006).

3.6 SoPIP2;1 – a plant aquaporin

Terrain plants evolved to cope with rapid changes in the availability of water by regulating AQPs in their plasma membrane. Plasma membrane AQPs close either upon dephosphorylation of two conserved serine residues (one in cytosolic loop B and one in the C-terminal region) under conditions of drought stress (Johansson *et al.* 1996, 1998) or from the protonation of a conserved histidine residue in loop D following a drop in cytoplasmic pH due to anoxia during flooding (Tournaire-Roux *et al.* 2003). Recently, the structure of SoPIP2;1 from spinach was determined by X-ray crystallography both in an open and closed pore state (Tornroth-Horsefield *et al.* 2006). In both cases the water pore was filled with an unbroken line of seven hydrogen-bonded water molecules.

The most striking difference between the structure of SoPIP2;1 and that of other AQPs is the conformation of the cytoplasmic loop D connecting transmembrane helices 4 and 5 (Tornroth-Horsefield *et al.* 2006). Compared to other AQPs this loop is elongated in SoPIP2;1 and seems to be responsible for the gating mechanism that opens and closes the water pore (see Section 6.3).

3.7 AQPM – an archaebacterial aquaporin

AQPM was discovered in the methanogenic archaebacterium *Methanothermobacter marburgensis*, confirming the presence of AQPs in archaea (Ding & Kitagawa, 2001). It was found to conduct water (Kozono *et al.* 2003) although at a very low rate (Lee *et al.* 2005). The structure of AQPM was determined to 1·68 Å resolution by X-ray crystallography showing unique features of pore architecture, implicating AQPM as a H_2S, CO_2 and H_2O conducting pore (Lee *et al.* 2005).

AQPM adopts the usual AQP fold, but unlike all other AQPs, loop A connecting transmembrane helices 1 and 2 is particularly long in AQPM, forming a hydrophobic pocket on the extracellular surface, in which glycerol and water molecules can bind (Fig. 11). The narrowest point in the AQPM pore is at the constriction site, formed by Arg202, Phe68, Ile187 and the carbonyl oxygen of Ser196. The topology of this constriction site is almost identical to that of other water selective AQPs. The only difference is that Ile187 replaces the histidine, which is highly conserved in water-selective AQPs, resulting in a slightly wider and more hydrophobic aperture than that of AQP1, accounting for the less efficient passage of water in AQPM.

The AQPM structure revealed four water molecules (HOH1–HOH4) and three glycerol molecules (G1–G3) lined up in a single file along the pore (Lee *et al.* 2005). Starting at the periplasmic vestibule, G1 occupies the first position at the mouth of the pore and is stabilized by hydrogen bonding between the hydroxyl group of C2-OH and the main chain carbonyl oxygen of Gly133. G3 is followed by three successive, hydrogen-bonded water molecules (HOH1–HOH3), located adjacent to the carbonyl oxygens of Gly195, Ser196 and Ser197, respectively. Following HOH3, G2 sits adjacent to the two NPA motifs of AQPM, followed by HOH4, which is stabilized by a hydrogen bond to the carbonyl oxygen of His80. G3 occupies the cytoplasmic vestibule of the pore. For a discussion of substrates for AQPM, see Section 5.

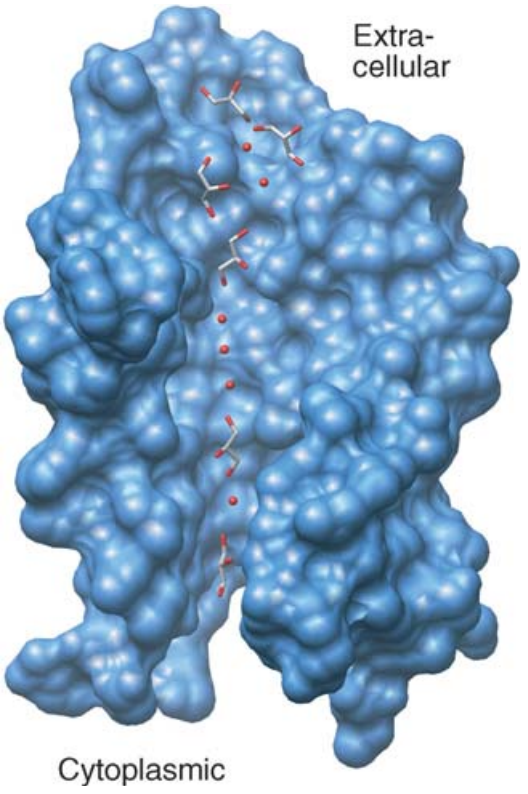

Fig. 11. The pore through AQPM. The AQPM pore contains glycerol molecules, but only water molecules occupy the constriction site in the middle of the pore. The extracellular loops form a hydrophobic pocket filled with glycerol molecules.

4. Proton exclusion

Despite their extreme water permeability – AQP1 allows permeation of 3×10^9 water molecules per monomer per second (Zeidel *et al.* 1992, 1994; Walz *et al.* 1994a) – AQPs strictly prevent the conduction of protons. This may be the most exceptional feature of AQPs, because continuous lines of hydrogen-bonded water molecules are excellent proton conductors. In these so-called 'proton wires' the charge of a proton can move from one end to the other by the Grotthuss mechanism, which is based on the simple switching of the hydrogen bonding pattern (Fig. 12) (Horne, 1964; Pomes & Roux, 1996, 1998; Cukierman, 2000). The crystal structure of AQP1 revealed a single file of six water molecules in the pore (Sui *et al.* 2001) and the GlpF structure determined in the absence of glycerol contained nine water molecules in the pore (Tajkhorshid *et al.* 2002). Similarly, one of the two AQPZ molecules in the asymmetric unit cell of the crystal contained five water molecules in the pore (Savage *et al.* 2003) and the open pore seen in the crystal structure of full-length AQP0 contained seven water molecules (Harries *et al.* 2004). So what prevents the conduction of protons along the line of water molecules in these AQP pores?

A first glimpse into the mechanism of proton exclusion was provided by the EM structure of AQP1, although water molecules were actually not resolved at the 3·8 Å resolution of the density map (Murata *et al.* 2000). The AQP1 structure showed that the two pore helices HB and HE are

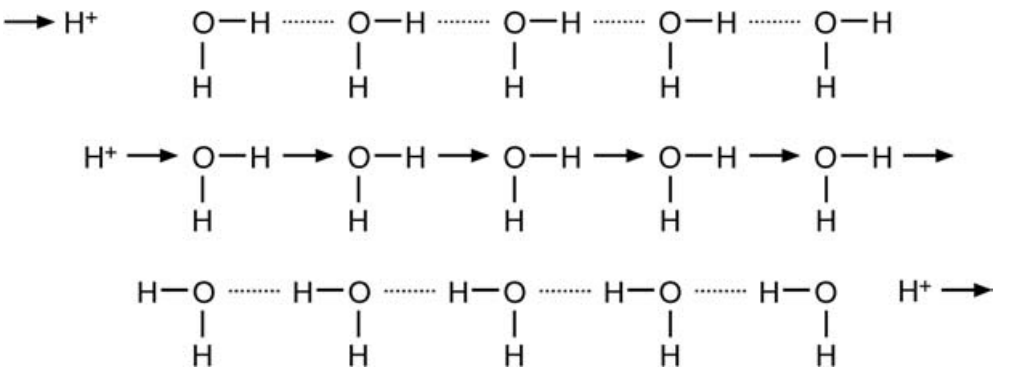

Fig. 12. The proton wire. Schematic representation of the Grotthuss mechanism, by which the charge of a proton can be transported along a continuous line of hydrogen-bonded water molecules.

oriented in opposite directions, with their C-termini facing away from the pore. The N-termini of the two pore helices are held together by proline–proline interactions of the NPA motifs close to the center of the water pore. The two Asn residues of the NPA motifs (Asn76 and Asn192 in AQP1) are held tightly in position and extend their side-chains into the pore. In this way the positive partial dipole moments of the two pore helices are focused into the amido groups of the NPA's Asn residues in the center of the pore. Based on this observation the 'hydrogen bond isolation mechanism' was proposed (Murata *et al.* 2000). In this model, a water molecule approaching the center of the pore would orient itself so that its oxygen atom can form hydrogen bonds with the side chains of the two Asn residues. As a result the two hydrogen atoms of the water molecule would be oriented perpendicular to the pore axis, preventing the formation of hydrogen bonds with neighboring water molecules in the pore. The isolation of this central water molecule in the pore would break the continuous line of hydrogen bonds and thus be a very efficient means to prevent protons from crossing the pore.

When the crystal structures of GlpF (Fu *et al.* 2000) and AQP1 (Sui *et al.* 2001) were determined, revealing the water molecules in the pore, a variety of computer simulation methods were used to study the dynamics of water molecules and the mobility of protons in AQP pores (recently reviewed in de Groot & Grubmuller, 2005). These simulations confirmed that the asparagine residues of the two NPA motifs indeed orient the water molecule in the center of the pore perpendicular to the pore axis. According to the simulations, the central water is still capable of forming hydrogen bonds with the neighboring water molecules, but it can only engage in hydrogen bonding leading outwards from the center of the pore towards the extracellular and the cytoplasmic entrance of the pore. The lines of water molecules in the two pore halves thus have opposite hydrogen bond polarity, preventing protons to cross the central water but allowing neutral solutes to permeate (Fig. 13). Recent mutation experiments also showed that removal of the positive charge from the ar/R constriction site in two AQP1 mutants, Arg195Val and His180Ala/Arg195Val, appeared to allow the passage of protons through the AQP1 pore (Beitz *et al.* 2006). The electrostatic proton barrier in AQPs thus appears to involve not only the NPA motifs but also the ar/R constriction site. In addition, the crystal structure of AQP1 revealed an arginine residue at the extracellular vestibule and histidine residues located in the cytoplasmic vestibule. The positive charges of these residues would help to repel protons from entering the pore (Sui *et al.* 2001). Two charged residues, Arg206 and Glu152, were also seen in

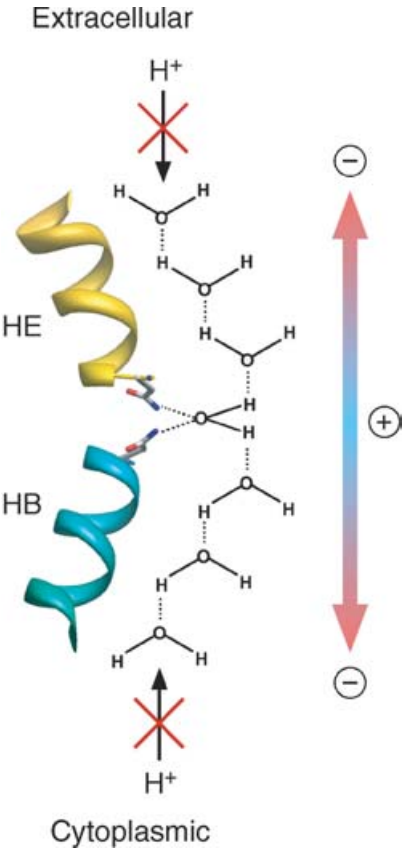

Fig. 13. The proton exclusion mechanism. The asparagine residues of the two NPA motifs orient the water molecule in the center of the pore with the two hydrogen atoms perpendicular to the pore axis, dividing the pore into two half channels. The electrostatic field in the pore causes the water molecules in the two half channnels to be oriented in opposite directions, thus preventing proton conduction through the pore.

the extracellular vestibule in the GlpF structure, where they may also impose electrostatic energy barriers, preventing the passage of charged molecules, including OH^- or H_3O^+. These two residues are conserved almost across all AQPs, suggesting that this may be a general mechanism used by members of the AQP family (Stroud *et al.* 2003a, b).

In the structure of the closed water pore in junctional AQP0 (Gonen *et al.* 2005) only three water molecules remain in the pore: the central water and the two neighboring ones in the extracellular and cytoplasmic halves of the pore, the first water molecules in the two lines of water molecules with opposite hydrogen bond polarity. In this way, the proton exclusion mechanism is maintained even in the closed water pore. In addition, the three water molecules are too far apart from each other to form hydrogen bonds, thus preventing the formation of a proton wire and further preventing proton conduction.

5. Substrate selectivity

While all AQPs conduct water but not protons, differences exist in their permeability to other uncharged solutes. The structures of the pure water pores AQP1, AQPZ, AQP0, and AQP4, the

glycerol facilitator GlpF and most recently the archaebacterial AQPM made it possible to understand the structural basis for the substrate selectivity of these different AQPs.

Water specificity in AQPs is due to the ar/R constriction site, which is located just above the two NPA motifs and narrows the pore in AQP1 to a diameter of about 3 Å, which is only slightly larger than the 2·8 Å diameter of a water molecule. GlpF conducts water and small, uncharged organic molecules, such as urea, glycine and glycerol whereas cyclized alditols (aldoses) are not conducted through the GlpF pore (reviewed in Stroud *et al.* 2003a, b). Pore profiles calculated for GlpF and AQP1 indicate that the pore of GlpF is larger (Sui *et al.* 2001), allowing molecules larger than water to permeate the GlpF pore. A number of substitutions in residues forming the constriction site of GlpF facilitate this. His182 of human AQP1 is replaced by a much smaller Gly191, allowing room for two additional substitutions: Cys191 of AQP1 to a much more hydrophobic Phe200, and Phe58 of AQP1 to a much larger Trp48 (Fu *et al.* 2000; Sui *et al.* 2001). The resulting constriction site has a larger diameter of 3·8 Å and is thus large enough to accommodate a glycerol molecule (Fu *et al.* 2000). A recent mutational analysis of the ar/R constriction site in rat AQP1 corroborated the notion of solute discrimination by size. Individual or joint substitutions of the His and Arg residues of the ar/R constriction site by Ala and Val residues, respectively (His180Ala, Arg195Val, and His180Ala/Arg195Val), did not affect water permeability, but the double mutant allowed urea permeation (Beitz *et al.* 2006). The double mutation Phe56Ala/His180Ala enlarged the maximal diameter of the ar/R constriction site 3-fold and made the pore permeable to glycerol and urea (Beitz *et al.* 2006). All four AQP mutants also allowed conduction of ammonia. Interestingly, removal of the positive charge in the ar/R constriction site of AQP1 (Arg197Val and His180Ala/Arg195Val) resulted in some proton leakage (Beitz *et al.* 2006).

The GlpF structure showed three glycerol molecules in the pore (G1–G3) (Fu *et al.* 2000) (Fig. 14). G1 is hydrogen-bonded to the oxygen of Tyr138 in the extracellular vestibule of GlpF while G2 and G3 are tightly held within the pore of GlpF. This region is only large enough to accommodate a single CH–OH group indicating that alditol molecules can only pass in a single file. Trapped water molecules in between G2 and G3 indicate that water may be co-transported with glycerol (Fu *et al.* 2000). Substitutions in constriction site residues in GlpF compared with AQP1 (see above) result in a highly amphipathic region, with the planes of Trp48 and Phe200 forming a hydrophobic corner, in which the alkyl backbone of G2 is tightly packed. In addition, G2 is in contact with Arg206 opposite the hydrophobic corner with two NHs guanidinium side chains of Arg206 serving as hydrogen bond donors to two successive OH groups of the glycerol (OH1 and OH2), while two main chain carbonyl oxygens from Gly199 and Phe200 serve as hydrogen bond acceptors to these OH groups. These elements result in a tripathic pore (Fu *et al.* 2000) composed of a hydrophobic corner, hydrogen bond donors and hydrogen bond acceptors. This pore topology ensures a tight fit for G2 at this site leaving no space for any substitutions at the COH hydrogen positions. G3 lies opposite the two NPA motifs of GlpF, interacting with the NH_2 groups of Asn68 and Asn203 from helices HB and HE. The NH_2 group of Asn203 is a donor to OH_1 of G3 and that of Asn68 to OH_2 of G3.

The structures of GlpF with and without glycerol are very similar (Tajkhorshid *et al.* 2002). In the absence of glycerol, GlpF contains nine water molecules in the pore, forming a continuous line through the entire pore. The most significant difference between the two structures lies in the orientation of three of the four constriction site residues, Trp48, Phe200, and Arg206, the position where G2 would bind. In the water bound state, these residues position their side-chains closer to each other, forming a narrower pore diameter, indicating a close interaction between

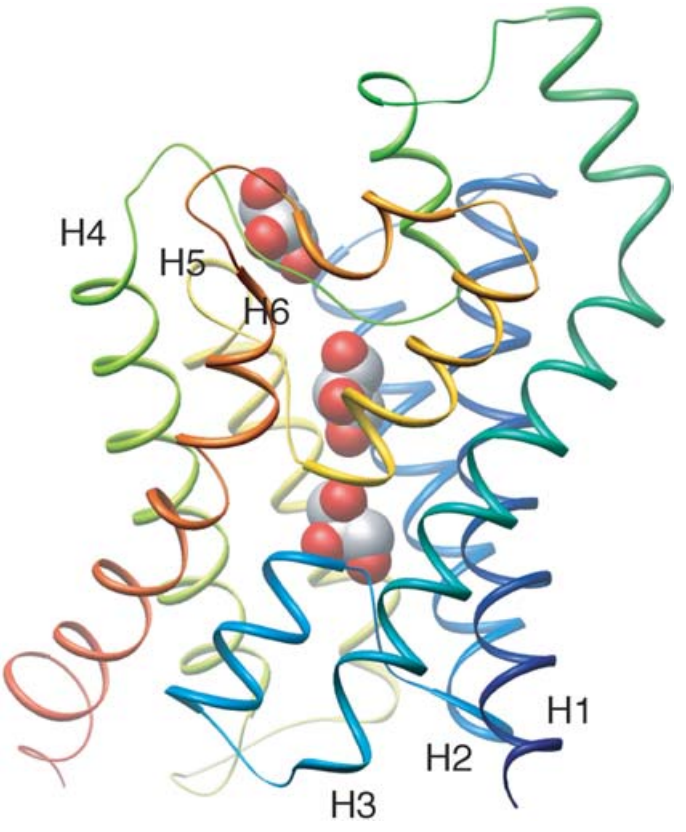

Fig. 14. Glycerol molecules in the GlpF pore. Ribbon diagram of GlpF containing three glycerol molecules shown in space-filling representation. The glycerol molecule in the center occupies the constriction, while the lowest one is located at the height of the two NPA motifs.

glycerol and pore at the constriction site (Tajkhorshid *et al.* 2002). Therefore, glycerol molecules can pass through the pore only with successive CHOH groups within one molecule following each other in a single file, explaining why the linear sugar ribitol shows a 10-fold increase in permeability compared with D-arabitol, a chiral stereoisomer of ribitol with a mixed arrangement of hydroxyls (Fu *et al.* 2000; reviewed in Stroud *et al.* 2003a, b).

The hydrophobic wall created by Trp48 and Phe200 at the constriction site of GlpF, may impair the permeation of water through the pore, and indeed GlpF is known to have lower conductivity for water compared with other AQPs (Maurel *et al.* 1994). In water-specific AQPs, Trp48 is typically replaced by a His residue while Phe200 is replaced by an Ala, Thr or Cys residue, creating a constriction site that allows a greater degree of water coordination than in GlpF. Mutation of the Trp48 to a Phe together with mutation of Phe200 to a Thr resulted in higher water conductivity through GlpF (Borgnia & Agre, 2001) and the electron density data for mutant GlpF indicated a significant increase of water density at the constriction site as compared to native GlpF (Tajkhorshid *et al.* 2002). Thus the presence of Trp48 and Phe200 in GlpF are vital for substrate selectivity, creating the hydrophobic corner needed for the coordination of a glycerol at the constriction site.

Structural studies on AQPM produced two crystal structures (Lee *et al.* 2005). In the lower resolution structure (2·3 Å) the pore contained almost exclusively water molecules (with one

glycerol in the NPA region), whereas the higher resolution structure (1·68 Å) revealed four water and three glycerol molecules in the pore. Functional studies showed that AQPM can conduct glycerol *in vitro* at a low rate (Kozono *et al.* 2003), but since *Methanothermobacter marburgensis* uses CO_2 as its sole carbon source (Smith *et al.* 1997), glycerol conduction is unlikely to be a biologically significant function of AQPM. Accordingly, the ar/R constriction site contains only water molecules in both structures. The presence of glycerol in the pore may be explained by the high concentration of glycerol in the crystallization buffer.

The ar/R constriction site in AQPM is similar to that of water-specific AQPs with the notable exception that Ile187 replaces the histidine residue that is otherwise fully conserved in water-selective AQPs. This substitution makes the constriction site in AQPM larger and more hydrophobic than in water-selective AQPs, but not as large and hydrophobic as in the glycerol facilitator GlpF. The substitution of this histidine residue by an aliphatic residue is also seen in other archaebacteria (Lee *et al.* 2005), which thus appear to constitute another AQP subgroup with a substrate specificity that lies in between those of water-specific AQPs and glycerol-conducting AQPs, possibly also allowing conducatnce of H_2S and CO_2 in addition to water. Since H_2S is very similar to H_2O, the selectivity mechanism is likely to be essentially the same (Lee *et al.* 2005).

6. Pore regulation

To maintain homeostasis it is essential for cells to tightly regulate the water permeability of their membranes. Members of the AQP family are thus regulated in a number of different ways to ensure that their permeability characteristics match the physiological requirements.

6.1 Hormonal regulation of AQP trafficking

Since the 1960s it was known that vasopressin causes a fast increase in water permeability in the collecting duct epithelium (Grantham & Burg, 1966; Morgan & Berliner, 1968), although it was not until the early 1990s that its target was identified as AQP2 (Zhang *et al.* 1993b). The process involves shuttling (Wade *et al.* 1981) of AQP2 from intracellular storage vesicles to the apical plasma membrane (Nielsen *et al.* 1995) and is reversed by inhibition of the hormone (Saito *et al.* 1997). This 'shuttle hypothesis' (Wade *et al.* 1981) was directly tested by labeling of AQP2 in intracellular vesicles that redistributed to the apical plasma membrane following application of vasopressin (Nielsen *et al.* 1995). The shuttling process involves several steps including translocation of vesicles to the cell apex; priming of vesicles and fusion with the apical plasma membrane believed to occur *via* clathrin coated pits (Brown & Orci, 1983; Strange *et al.* 1988; Rapaport *et al.* 1997). A comprehensive review of the role of AQPs in the kidney is provided in Knepper *et al.* (2001), and Deen & Brown (2001) have reviewed the trafficking of AQPs.

Other AQPs are also regulated by hormones. AQP1 water permeability increases with vasopressin and decreases with atrial natriuretic peptide, a peptide hormone that plays an important role in the regulation of body fluid homeostasis (Patil *et al.* 1997). Incubation of oocytes with 8-bromo cAMP, a membrane permeable cAMP analog, or vasopressin was found to increase the abundance of AQP1 in the plasma membrane (Han & Patil, 2000). A redistribution of AQP1 from intracellular stores to the apical membrane of cholangiocytes was

observed in experiments done on bile duct epithelial cells using secretin, a hormone that stimulates ductal bile secretion (Marinelli *et al.* 1997, 1999). The activity of AQP4 in brain cells is also stimulated by vasopressin. In primary cultures of astrocytes, vasopressin was reported to increase the rate of cell swelling in hypotonic medium (Sarfaraz & Fraser, 1999). Under basal conditions, cell surface AQP8 expression is very low in hepatocytes with most of the protein found in vesicular compartments inside the cell, indicating only a small contribution of this AQP to the total hepatocyte membrane water permeability (Yano *et al.* 1996; Calamita *et al.* 2001; Garcia *et al.* 2001; Huebert *et al.* 2002; Gradilone *et al.* 2003). However, upon stimulation with the hormone glucagon or its secondary messenger cAMP, intracellular AQP8 redistributes to the plasma membrane causing an increase in cell surface water permeability (Garcia *et al.* 2001; Huebert *et al.* 2002; Gradilone *et al.* 2003; Marinelli *et al.* 2003). Hormone-induced redistribution of AQPs from intracellular storages thus appears to be a generally used mechanism to regulate water permeability of the plasma membrane in a number of different tissues and cell types.

6.2 Influence of pH on AQP water conduction

The permeability characteristics of some AQPs, including AQP3 (Zeuthen & Klaerke, 1999), AQP6 (Yasui *et al.* 1999a), and AQP0 (Nemeth-Cahalan & Hall, 2000), were shown to be sensitive to pH. AQP3 confers permeability to water and glycerol at neutral pH but appears to be closed at a pH <6 (Zeuthen & Klaerke, 1999). In contrast, AQP6 only opens at a pH of $\leqslant 5{\cdot}5$, allowing selective permeation of water and chloride ions (Yasui *et al.* 1999a; Hazama *et al.* 2002; Liu *et al.* 2005).

AQP0 water permeability is maximum at the slightly acidic pH of 6·5 (Nemeth-Cahalan & Hall, 2000). His40 in loop A was identified as possible pH sensor, because it is the only His residue present in AQP0 but not in AQP1, which is not sensitive to pH. His40 was then shown to be involved in pH regulation both in oocytes expressing AQP0 (Nemeth-Cahalan & Hall, 2000) and in lens fiber cells (Varadaraj *et al.* 2005). Additionally, AQP1 water permeability could be made pH sensitive by introducing His residues into loop A of this protein (Nemeth-Cahalan *et al.* 2004). Furthermore, the pH of maximum water conduction can be shifted towards a more alkaline or acidic pH by changing the exact position of this residue in AQP0. For example, in the kilifish homolog of AQP0, the histidine in loop A is at position 39, and water permeability is maximal at an alkaline rather than an acidic pH. Moving His39 to position 40 (His39Leu/Asn40His) shifted the pH sensitivity back into the acidic range. In addition to the His residue in loop A, other residues have also been implicated in pH regulation. The atomic structure of AQP0 showed that two His residues, His40 and His66, are at positions, where they could influence water conductance (Gonen *et al.* 2004a). His40, already previously implicated in pH dependence of AQP0 water conductance, is located at the extracellular entrance of the pore and its side-chain extends into the water pathway. Hence, protonation or deprotonation of His40 could be one mechanism by which pH influences AQP0 water permeation. The second His residue, His66, is part of constriction site II in AQP0, formed by Tyr149, Phe75 and His66. The side-chains of these three residues extend into the water pathway and may constitute a pH-regulated gate, with Tyr149 acting as the flap and His66 as the pH sensor (Gonen *et al.* 2004a; Gonen *et al.* 2005). While His40 in loop A of AQP0 is firmly established in pH regulation, further experiments are needed to determine the true contribution of other residues implicated in pH regulation, such as His66.

6.3 Regulation of AQP pore conductance by protein binding

Binding of proteins to AQPs appears to be another strategy by which their permeability characteristics can be regulated. The activity of AQP0 is regulated by the Ca^{2+} concentration (Nemeth-Cahalan & Hall, 2000). In oocytes, a low Ca^{2+} concentration caused an increase in AQP0 water permeability (Nemeth-Cahalan *et al.* 2004). By contrast, in isolated vesicles, it was an increase in Ca^{2+} concentration that resulted in an increase in water permeability of up to 4-fold (Varadaraj *et al.* 2005). This increase in water permeability was mediated by calmodulin. Calmodulin inhibitors (Nemeth-Cahalan *et al.* 2004) or a calmodulin mutant (Varadaraj *et al.* 2005) abolished the increase in water permeability following changes in Ca^{2+} concentration. Since they did not alter the increase in water permeability produced by acidic pH, the regulation of AQP0 pore activity by pH and by Ca^{2+} are two independent processes.

The Ca^{2+}-dependent increase in water permeability is mediated by binding of calmodulin to the distal part of the AQP0 C-terminus (Varadaraj *et al.* 2005). How does this effect relate to the age-related truncation of the AQP0 C-terminus in the lens (Roy *et al.* 1979; Takemoto *et al.* 1986; Zampighi *et al.* 1989)? The cleavage causes AQP0 to form junctions (Kistler & Bullivant, 1980; Gonen *et al.* 2004b), in which the pores are closed (Gonen *et al.* 2004a, 2005). It may be that binding of calmodulin to the remaining non-junctional AQP0 molecules increases their water permeability, thus compensating for the fraction of AQP0 molecules lost to the membrane junctions. Alternatively, calmodulin binding to the C-terminus of AQP0 may constitute a mechanism by which the lens ensures that a certain fraction of AQP0 is protected from cleavage and therefore are not engaged in junction formation. Further experiments are needed to determine the physiological relevance of calcium/calmodulin regulation of AQP0 pore activity.

Water conductance of plant SoPIP2;1 is regulated by the phosphorylation of two conserved serine residues, Ser247 and Ser115 (Johansson *et al.* 1996, 1998) and by the protonation of a conserved His residue (Tournaire-Roux *et al.* 2003). Structures of SoPIP2;1 in the open and closed pore state revealed that the gating of the pore is mediated by loop D (Tornroth-Horsefield *et al.* 2006). In the closed conformation loop D folds underneath the protein occluding the water pore from accessing the cytosol, and placing Leu197 from loop D into a cavity near the entrance of the pore (Fig. 15). In addition to Leu197, residues His99, Val104 and Leu108 form a hydrophobic barrier that narrows the pore diameter to 1·4 Å at Leu197, and to 0·8 Å near residues Pro195 and Val194. In the structure of SoPIP2;1 in the open state, loop D is displaced up to 16 Å and the N-terminus of helix 5 extends a further half-turn into the cytoplasm, resulting in displacement of the Cα atoms of Leu197, Pro195 and Val194 away from the pore entrance by 8·4 Å, 13·9 Å and 15 Å respectively. These structural changes increase the pore diameter to more than 4 Å. Interestingly, Leu197 of SoPIP2;1 in the closed conformation overlays almost perfectly with Tyr149 from AQP0, a residue implicated in forming a pH gate (Gonen *et al.* 2004a).

Phosphorylation and dephosphorylation of Ser247 and Ser115 affect pore opening and closure, respectively. Dephosphorylated Ser274 interacts with the backbone nitrogens of Pro199 and Leu200 of an adjacent monomer in the closed pore state. When Ser247 is phosphorylated these interactions are lost, loop D is displaced and Leu197 occupies the position previously taken by Ser247. This allows the N terminus of helix 5 to extend another half-turn into the cytoplasm, thereby displacing the Leu197 and opening the water pore. In the

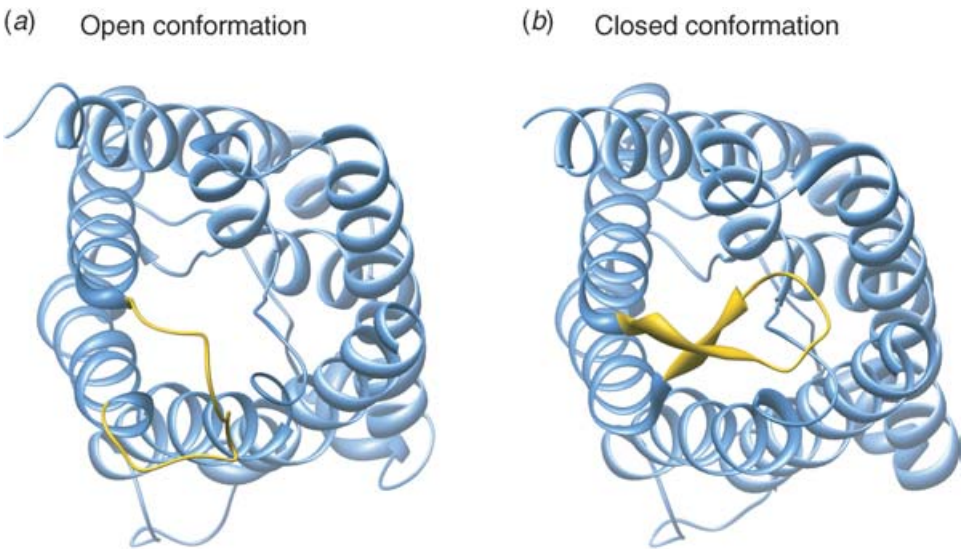

Fig. 15. Open and closed conformations of the SoPIP2;1 water pore. (*a*) In the open conformation, cytoplasmic loop D (yellow) is displaced from the opening of the water pore. (*b*) In the closed conformation, loop D blocks the entrance of the pore and abolishes water conduction.

closed pore conformation loop D is anchored to the N terminus by a network of hydrogen bonding involving dephosphorylated Ser115, Asp28, Glu31 and the mobile residues from loop D (Ser188–Ala198). Phosphorylation of Ser115 disrupts these interactions, releasing loop D and allowing it to become displaced resulting in pore opening. The mechanism of pore closure and opening were confirmed by molecular dynamic simulations (Tornroth-Horsefield *et al.* 2006). Protonation of His193 in SoPIP2;1 (strictly conserved in plant plasma membrane AQPs) was also shown to close the pore (Tournaire-Roux *et al.* 2003). A rotation of this histidine residue in the protonated state would allow it to form a salt bridge to Asp28 (conserved in plant plasma membrane AQPs as Asp or Glu). This would recover the anchor for loop D on the N terminus, which is lost upon phosphorylation of Ser115 and would thus result in the same closed pore conformation observed in the crystal structure (Tornroth-Horsefield *et al.* 2006).

In AQP4, phosphorylation of Ser180 has been implicated in protein kinase C- and dopamine-dependent decrease in AQP4 water permeability (Zelenina *et al.* 2002). Ser180 is located close to the cytoplasmic opening of the AQP4 pore. Possibly the phosphorylation of Ser180 leads to the recruitment of a protein that blocks the water pore. Similar to SoPIP2;1, one possibility would be that the C-terminal domain of AQP4 itself binds to phosphorylated Ser180, in which case the interaction could be mediated by positively charged amino-acid residues (Lys259, Arg260 and Arg261) present in the C-terminus.

6.4 Pore closure by conformational changes in the AQP pore

AQP conduction can also be regulated by closure of the pore through conformational changes in pore-lining residues. The structure of AQP0 was determined in an open state by X-ray crystallography of detergent-solubilized tetramers (Harries *et al.* 2004) as well as in a closed

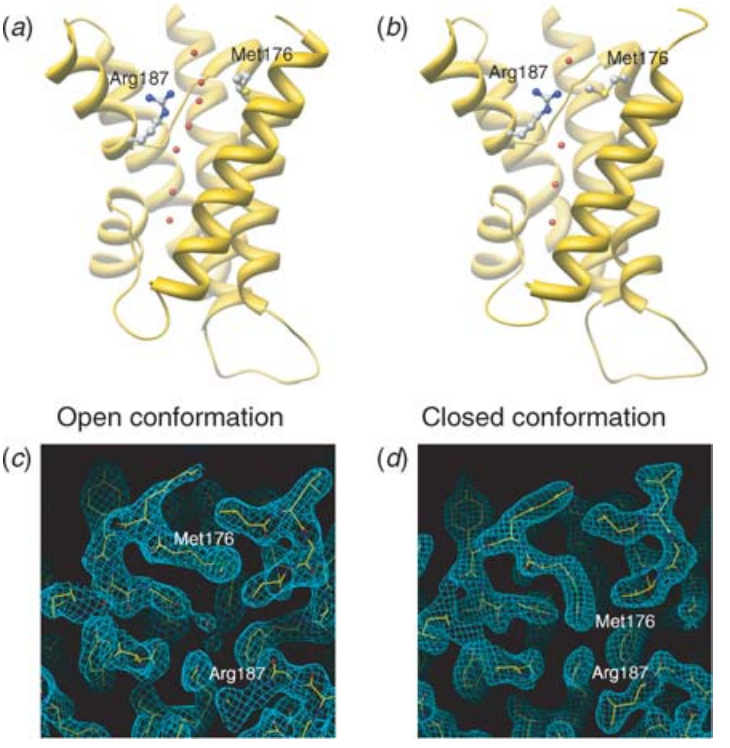

Fig. 16. Open and closed conformations of the AQP0 water pore. (*a*, *b*) In the open conformation, the side-chain of Met176 is pointing away from the pore allowing a continuous line of water molecules to form (*a*), whereas in the closed conformation the side-chain extends into the pore and displaces three water molecules (*b*). The conformation of Arg187 is the same in the open and closed states. (*c*, *d*) Density maps looking into the water pore from the extracellular surface, revealing two of the water molecules in the open pore (*c*) that are displaced upon the conformational change in Met176 (*d*).

state by electron crystallography of double-layered 2D crystals (Gonen *et al.* 2004a, 2005). Comparison of the two structures revealed the structural differences between the two pore states (Fig. 16).

Truncation of the AQP0 termini alone is unlikely to be responsible for the closed pore conformation, because it has been shown previously not to affect water conductance (Ball *et al.* 2003). AQP0 water conductance is pH-dependent with a maximum at pH 6·5 and only about half the activity at pH 10·5 (Nemeth-Cahalan *et al.* 2004). Although the double-layered 2D crystals were grown at pH 6 (Gonen *et al.* 2004a, 2005), the water pore contains less water molecules in the pore than the structure produced with the 3D crystals grown at pH 10·5 (Harries *et al.* 2004). This suggests that neither truncation nor pH but junction formation between apposing AQP0 tetramers is responsible for the stabilization of the pore in the closed conformation. The two pores have similar diameters over much of their lengths, but the pore in junctional AQP0 is narrower at the positions of the two constriction sites. CS-I in non-junctional AQP0 spans 3 Å and has a minimum diameter of 2·31 Å (Gonen *et al.* 2005). In junctional AQP0, CS-I extends over almost 10 Å and the pore narrows to 1·33 Å. CS-II is also narrower in junctional AQP0 (diameter 1·37 Å) than in non-junctional AQP0 (diameter 1·75 Å).

Initially, it was proposed that Arg187, part of CS-I, may be the gate responsible for pore closure in AQP0, because its side chain was in a different conformation than those of the corresponding arginine residues in almost all other AQP structures (Gonen *et al.* 2004a). This notion was supported by studies on AQPZ. The crystal structure of AQPZ showed two protomers (A and B) in the asymmetric unit (Savage *et al.* 2003). Arg189 in the constriction site of protomer A adopted the conventional 'UP' conformation seen in most AQPs, and the pore was filled with water molecules. By contrast, Arg189 in protomer B adopted the conformation seen in the structure of junctional AQP0, referred to as 'DOWN' state, and the water pore contained only three water molecules. Molecular dynamics experiments on AQPZ showed that Arg189 can flip between the two conformations, and that the 'UP' state would correspond to an open pore, whereas the pore in the 'DOWN' state would be closed (Wang *et al.* 2005). Meanwhile, another crystal structure for AQPZ showed the two different conformations of Arg189 in different subunits of the same tetramer, leading the authors to suggest that the different conformations are related to water permeation through the ar/R constriction site of the pore rather than to pore closure (Jiang *et al.* 2006). When the structure of AQP0 was determined in the open state (Harries *et al.* 2004), Arg187 adopted essentially the same conformation as in the structure of the closed pore (Gonen *et al.* 2004a), also suggesting that a conformational switch in Arg187 might not be the predominant reason for pore closure in AQP0. The 1·9 Å structure of junctional AQP0 (Gonen *et al.* 2005) then revealed that the main difference between open and closed pore lies in the conformation of the side-chain of Met176 (Fig. 16), a residue not present in AQPZ. While it is clear that Met176 obstructs the water pathway in the closed AQP0 pore, further studies will be required to understand how junction formation triggers the conformational change in the side chain of Met176.

7. Unresolved questions

The many structures now available for members of the AQP family have provided a tremendous amount of insight into the function and regulation of these membrane pores. However, many questions still remain. The most intriguing question concerns the central cavity in the AQP tetramer. While each monomer forms an independent water pore, every AQP studied to date forms a tetramer, which contains a large, water and proton impermeable cavity. So far, no function has been assigned to this intriguing pore-like structure, but it has been speculated to function as an ion or gas channel. The biological functions of AQPs 11 and 12 remain to be identified, and a structure for AQP6 would be essential to understand how it can conduct anions and why it is activated rather than inhibited by mercurials. The structural features that define whether an AQP is permeable to CO_2 or not are unclear, and many of the mechanistic details how pH and phosphorylation regulate pore characteristics remain to be elucidated. While all AQPs share the same basic fold, it is the subtle differences between the different AQPs that provided most of the insights. As functional and structural studies on AQPs continue and are combined with computer simulations, we can look forward to further discoveries that will help us understand general characteristics of membrane pores, such as substrate selectivity and regulation of pore characteristics.

8. Acknowledgments

Work on aquaporins in the Walz laboratory is supported by NIH funding.

9. References

Agre, P., Borgnia, M., Yasui, M., Neely, J., Carbrey, J., Kozono, D., Beitz, E., Hoffert, J., Leitch, V. & King, L. S. (2001). Discovery of the aquaporins and their impact on basic and clinical physiology. In Hohmann, S., Nielsen, S. & Agre, P. (eds.), *Aquaporins*, vol. 51, pp. 1–38. San Diego: Academic Press.

Agre, P. & Kozono, D. (2003). Aquaporin water channels: molecular mechanisms for human diseases. *FEBS Letters* **555**, 72–78.

Agre, P., Saboori, A. M., Asimos, A. & Smith, B. L. (1987). Purification and partial characterization of the Mr 30,000 integral membrane protein associated with the erythrocyte Rh(D) antigen. *Journal of Biological Chemistry* **262**, 17497–17503.

Agre, P., Sasaki, S. & Chrispeels, M. J. (1993). Aquaporins: a family of water channel proteins. *American Journal of Physiology* **265**, F461.

Alcala, J., Lieska, N. & Maisel, H. (1975). Protein composition of bovine lens cortical fiber cell membranes. *Experimental Eye Research* **21**, 581–595.

Ball, L. E., Little, M., Nowak, M. W., Garland, D. L., Crouch, R. K. & Schey, K. L. (2003). Water permeability of C-terminally truncated aquaporin 0 (AQP0 1-243) observed in the aging human lens. *Investigative Ophthalmology and Visual Sciences* **44**, 4820–4828.

Beitz, E., Wu, B., Holm, L. M., Schultz, J. E. & Zeuthen, T. (2006). Point mutations in the aromatic/arginine region in aquaporin 1 allow passage of urea, glycerol, ammonia, and protons. *Proceedings of the National Academy of Sciences USA* **103**, 269–274.

Bloemendal, H., Zweers, A., Vermorken, F., Dunia, I. & Benedetti, E. L. (1972). The plasma membranes of eye lens fibres. Biochemical and structural characterization. *Cell Differentiation* **1**, 91–106.

Bok, D., Dockstader, J. & Horwitz, J. (1982). Immunocytochemical localization of the lens main intrinsic polypeptide (MIP26) in communicating junctions. *Journal of Cell Biology* **92**, 213–220.

Borgnia, M., Nielsen, S., Engel, A. & Agre, P. (1999). Cellular and molecular biology of the aquaporin water channels. *Annual Reviews in Biochemistry* **68**, 425–458.

Borgnia, M. J. & Agre, P. (2001). Reconstitution and functional comparison of purified GlpF and AqpZ, the glycerol and water channels from Escherichia coli. *Proceedings of the National Academy of Sciences USA* **98**, 2888–2893.

Brown, D. & Orci, L. (1983). Vasopressin stimulates formation of coated pits in rat kidney collecting ducts. *Nature* **302**, 253–255.

Calamita, G., Mazzone, A., Bizzoca, A., Cavalier, A., Cassano, G., Thomas, D. & Svelto, M. (2001). Expression and immunolocalization of the aquaporin-8 water channel in rat gastrointestinal tract. *European Journal of Cell Biology* **80**, 711–719.

Chandy, G., Zampighi, G. A., Kreman, M. & Hall, J. E. (1997). Comparison of the water transporting properties of MIP and AQP1. *Journal of Membrane Biology* **159**, 29–39.

Cheng, A., van Hoek, A. N., Yeager, M., Verkman, A. S. & Mitra, A. K. (1997). Three-dimensional organization of a human water channel. *Nature* **387**, 627–630.

Chepelinsky, A. B. (2003). The ocular lens fiber membrane specific protein MIP/Aquaporin 0. *Journal of Experimental Zoology, part A: Comparative Experimental Biology* **300**, 41–46.

Costello, M. J., McIntosh, T. J. & Robertson, J. D. (1989). Distribution of gap junctions and square array junctions in the mammalian lens. *Investigative Ophthalmology and Visual Science* **30**, 975–989.

Cukierman, S. (2000). Proton mobilities in water and in different stereoisomers of covalently linked gramicidin A channels. *Biophysical Journal* **78**, 1825–1834.

de Groot, B. L. & Grubmuller, H. (2005). The dynamics and energetics of water permeation and proton exclusion in aquaporins. *Current Opinion in Structural Biology* **15**, 176–183.

Deen, P. M. & Brown, D. (2001). Trafficking of native and mutant mammalian MIP proteins. In Hohmann, S., Nielsen, S. & Agre, P. (eds.), *Aquaporins*, vol. 51, pp. 235–276. San Diego: Academic Press.

Ding, X. & Kitagawa, Y. (2001). Rapid amplification of a water channel-like gene and its flanking sequences from the Methanothermobacter marburgensis genome using a single primer PCR strategy. *Journal of Bioscience and Bioengineering* **92**, 488–491.

Doyle, D. A., Morais Cabral, J., Pfuetzner, R. A., Kuo, A., Gulbis, J. M., Cohen, S. L., Chait, B. T. & MacKinnon, R. (1998). The structure of the potassium channel: molecular basis of K^+ conduction and selectivity. *Science* **280**, 69–77.

Drake, K. D., Schuette, D., Chepelinsky, A. B., Jacob, T. J. & Crabbe, M. J. (2002). pH-Dependent channel activity of heterologously-expressed main intrinsic protein (MIP) from rat lens. *FEBS Letters* **512**, 199–204.

Dunia, I., Manenti, S., Rousselet, A. & Benedetti, E. L. (1987). Electron microscopic observations of reconstituted proteoliposomes with the purified major intrinsic membrane protein of eye lens fibers. *Journal of Cell Biology* **105**, 1679–1689.

Ehring, G. R., Zampighi, G., Horwitz, J., Bok, D. & Hall, J. E. (1990). Properties of channels reconstituted from the major intrinsic protein of lens fiber membranes. *Journal of General Physiology* **96**, 631–664.

Fischbarg, J., Kuang, K. Y., Vera, J. C., Arant, S., Silverstein, S. C., Loike, J. & Rosen, O. M. (1990). Glucose transporters serve as water channels. *Proceedings of the National Academy of Sciences USA* **87**, 3244–3247.

Fotiadis, D., Hasler, L., Muller, D. J., Stahlberg, H., Kistler, J. & Engel, A. (2000). Surface tongue-and-groove contours on lens MIP facilitate cell-to-cell adherence. *Journal of Molecular Biology* **300**, 779–789.

Fu, D., Libson, A., Miercke, L. J., Weitzman, C., Nollert, P., Krucinski, J. & Stroud, R. M. (2000). Structure of a glycerol-conducting channel and the basis for its selectivity. *Science* **290**, 481–486.

Fujiyoshi, Y. (1998). The structural study of membrane proteins by electron crystallography. *Advances in Biophysics* **35**, 25–80.

Furman, C. S., Gorelick-Feldman, D. A., Davidson, K. G., Yasumura, T., Neely, J. D., Agre, P. & Rash, J. E. (2003). Aquaporin-4 square array assembly: opposing actions of M1 and M23 isoforms. *Proceedings of the National Academy of Sciences USA* **100**, 13609–13614.

Fushimi, K., Uchida, S., Hara, Y., Hirata, Y., Marumo, F. & Sasaki, S. (1993). Cloning and expression of apical membrane water channel of rat kidney collecting tubule. *Nature* **361**, 549–552.

Garcia, F., Kierbel, A., Larocca, M. C., Gradilone, S. A., Splinter, P., LaRusso, N. F. & Marinelli, R. A. (2001). The water channel aquaporin-8 is mainly intracellular in rat hepatocytes, and its plasma membrane insertion is stimulated by cyclic AMP. *Journal of Biological Chemistry* **276**, 12147–12152.

Gonen, T., Cheng, Y., Kistler, J. & Walz, T. (2004b). Aquaporin-0 membrane junctions form upon proteolytic cleavage. *Journal of Molecular Biology* **342**, 1337–1345.

Gonen, T., Sliz, P., Kistler, J., Cheng, Y. & Walz, T. (2004a). Aquaporin-0 membrane junctions reveal the structure of a closed water pore. *Nature* **429**, 193–197.

Gonen, T., Cheng, Y., Sliz, P., Hiroaki, Y., Fujiyoshi, Y., Harrison, S. C. & Walz, T. (2005). Lipid-protein interactions in double-layered two-dimensional crystals of aquaporin-0. *Nature* **438**, 633–638.

Gorin, M. B., Yancey, S. B., Cline, J., Revel, J. P. & Horwitz, J. (1984). The major intrinsic protein (MIP) of the bovine lens fiber membrane: characterization and structure based on cDNA cloning. *Cell* **39**, 49–59.

Gradilone, S. A., Carreras, F. I., Lehmann, G. L. & Marinelli, R. A. (2005). Phosphatidylinositol-3-kinase is involved in the glucagon-induced translocation of aquaporin-8 to hepatocyte plasma membrane. *Biology of the Cell* **97**, 831–836.

Gradilone, S. A., Garcia, F., Huebert, R. C., Tietz, P. S., Larocca, M. C., Kierbel, A., Carreras, F. I., Larusso, N. F. & Marinelli, R. A. (2003). Glucagon induces the plasma membrane insertion of functional aquaporin-8 water channels in isolated rat hepatocytes. *Hepatology* **37**, 1435–1441.

Grantham, J. J. & Burg, M. B. (1966). Effect of vasopressin and cyclic AMP on permeability of isolated collecting tubules. *American Journal of Physiology* **211**, 255–259.

Han, Z. & Patil, R. V. (2000). Protein kinase A-dependent phosphorylation of aquaporin-1. *Biochemical and Biophysical Research Communications* **273**, 328–332.

Hara-Chikuma, M. & Verkman, A. S. (2005). Aquaporin-3 functions as a glycerol transporter in mammalian skin. *Biology of the Cell* **97**, 479–486.

Harries, W. E., Akhavan, D., Miercke, L. J., Khademi, S. & Stroud, R. M. (2004). The channel architecture of aquaporin 0 at a 2.2-Å resolution. *Proceedings of the National Academy of Sciences of the United States of America* **101**, 14045–14050.

Harris Jr., H. W., Hosselet, C., Guay-Woodford, L. & Zeidel, M. L. (1992). Purification and partial characterization of candidate antidiuretic hormone water channel proteins of M(r) 55,000 and 53,000 from toad urinary bladder. *Journal of Biological Chemistry* **267**, 22115–22121.

Hasegawa, H., Ma, T., Skach, W., Matthay, M. A. & Verkman, A. S. (1994). Molecular cloning of a mercurial-insensitive water channel expressed in selected water-transporting tissues. *Journal of Biological Chemistry* **269**, 5497–5500.

Hasler, L., Walz, T., Tittmann, P., Gross, H., Kistler, J. & Engel, A. (1998). Purified lens major intrinsic protein (MIP) forms highly ordered tetragonal two-dimensional arrays by reconstitution. *Journal of Molecular Biology* **279**, 855–864.

Hazama, A., Kozono, D., Guggino, W. B., Agre, P. & Yasui, M. (2002). Ion permeation of AQP6 water channel protein. Single channel recordings after Hg^{2+} activation. *Journal of Biological Chemistry* **277**, 29224–29230.

Heller, K. B., Lin, E. C. & Wilson, T. H. (1980). Substrate specificity and transport properties of the glycerol facilitator of Escherichia coli. *Journal of Bacteriology* **144**, 274–278.

Hiroaki, Y., Kazutoshi, T., Kamegawa, A., Gyobo, N., Nishikawa, K., Suzuki, H., Walz, T., Sasaki, S., Mitsuoka, K., Kimura, K., Mizoguchi, A. & Fujiyoshi, Y. (2006). Implications of the aquaporin-4 structure on array formation and cell adhesion. *Journal of Molecular Biology* **355**, 628–639.

Horne, R. A. (1964). Role of the Grotthuss mechanism for protonic and electronic transport in the transmission of impulses along muscle fibres. *Nature* **202**, 1221.

Huebert, R. C., Splinter, P. L., Garcia, F., Marinelli, R. A. & LaRusso, N. F. (2002). Expression and localization of aquaporin water channels in rat hepatocytes. Evidence for a role in canalicular bile secretion. *Journal of Biological Chemistry* **277**, 22710–22717.

Ikeda, M., Beitz, E., Kozono, D., Guggino, W. B., Agre, P. & Yasui, M. (2002). Characterization of aquaporin-6 as a nitrate channel in mammalian cells. Requirement of pore-lining residue threonine 63. *Journal of Biological Chemistry* **277**, 39873–39879.

Ishibashi, K., Kuwahara, M., Gu, Y., Kageyama, Y., Tohsaka, A., Suzuki, F., Marumo, F. & Sasaki, S. (1997a). Cloning and functional expression of a new water channel abundantly expressed in the testis permeable to water, glycerol, and urea. *Journal of Biological Chemistry* **272**, 20782–20786.

Ishibashi, K., Kuwahara, M., Gu, Y., Tanaka, Y., Marumo, F. & Sasaki, S. (1998). Cloning and functional expression of a new aquaporin (AQP9) abundantly expressed in the peripheral leukocytes permeable to water and urea, but not to glycerol. *Biochemical and Biophysical Research Communications* **244**, 268–274.

Ishibashi, K., Kuwahara, M., Kageyama, Y., Sasaki, S., Suzuki, M. & Imai, M. (2000). Molecular cloning of a new aquaporin superfamily in mammals. In Hohmann, S. & Nielsen, S. (eds.), *Molecular Biology and Physiology of Water and Solute Transport*, pp. 123–126. New York: Kluwer Academic/Plenum Publishers.

Ishibashi, K., Kuwahara, M., Kageyama, Y., Tohsaka, A., Marumo, F. & Sasaki, S. (1997b). Cloning and functional expression of a second new aquaporin abundantly expressed in testis. *Biochemical and Biophysical Research Communications* **237**, 714–718.

Ishibashi, K., Morinaga, T., Kuwahara, M., Sasaki, S. & Imai, M. (2002). Cloning and identification of a new member of water channel (AQP10) as an aquaglyceroporin. *Biochimica et Biophysica Acta* **1576**, 335–340.

Jap, B. K. & Li, H. (1995). Structure of the osmo-regulated H2O-channel, AQP-CHIP, in projection at 3.5 Å resolution. *Journal of Molecular Biology* **251**, 413–420.

Jiang, J., Daniels, B. V. & Fu, D. (2006). Crystal structure of AqpZ tetramer reveals two distinct Arg-189 conformations associated with water permeation through the narrowest constriction of the water-conducting channel. *Journal of Biological Chemistry* **281**, 454–460.

Johansson, I., Karlsson, M., Shukla, V. K., Chrispeels, M. J., Larsson, C. & Kjellbom, P. (1998). Water transport activity of the plasma membrane aquaporin PM28A is regulated by phosphorylation. *Plant Cell* **10**, 451–459.

Johansson, I., Larsson, C., Ek, B. & Kjellbom, P. (1996). The major integral proteins of spinach leaf plasma membranes are putative aquaporins and are phosphorylated in response to Ca^{2+} and apoplastic water potential. *Plant Cell* **8**, 1181–1191.

Jung, J. S., Bhat, R. V., Preston, G. M., Guggino, W. B., Baraban, J. M. & Agre, P. (1994b). Molecular characterization of an aquaporin cDNA from brain: candidate osmoreceptor and regulator of water balance. *Proceedings of the National Academy of Sciences USA* **91**, 13052–13056.

Jung, J. S., Preston, G. M., Smith, B. L., Guggino, W. B. & Agre, P. (1994a). Molecular structure of the water channel through aquaporin CHIP. The hourglass model. *Journal of Biological Chemistry* **269**, 14648–14654.

King, L. S., Kozono, D. & Agre, P. (2004). From structure to disease: the evolving tale of aquaporin biology. *Nature Reviews Molecular Cell Biology* **5**, 687–698.

Kistler, J. & Bullivant, S. (1980). Lens gap junctions and orthogonal arrays are unrelated. *FEBS Letters* **111**, 73–78.

Knepper, M. A., Nielsen, S. & Chou, C. L. (2001). Physiological roles of aquaporins in the kidney. In Hohmann, S., Nielsen, S. & Agre, P. (eds.), *Aquaporins*, vol. 51, pp. 121–153. San Diego: Academic Press.

Kozono, D., Ding, X., Iwasaki, I., Meng, X., Kamagata, Y., Agre, P. & Kitagawa, Y. (2003). Functional expression and characterization of an archaeal aquaporin. AqpM from methanothermobacter marburgensis. *Journal of Biological Chemistry* **278**, 10649–10656.

Kushmerick, C., Rice, S. J., Baldo, G. J., Haspel, H. C. & Mathias, R. T. (1995). Ion, water and neutral solute transport in Xenopus oocytes expressing frog lens MIP. *Experimental Eye Research* **61**, 351–362.

Lee, J. K., Kozono, D., Remis, J., Kitagawa, Y., Agre, P. & Stroud, R. M. (2005). Structural basis for conductance by the archaeal aquaporin AqpM at 1.68 Å. *Proceedings of the National Academy of Sciences USA* **102**, 18932–18937.

Lee, M. D., King, L. S. & Agre, P. (1998). Aquaporin water channels in eye and other tissues. *Current Topics in Membranes* **45**, 105–134.

Li, H., Lee, S. & Jap, B. K. (1997). Molecular design of aquaporin-1 water channel as revealed by electron crystallography. *Nature Structural Biology* **4**, 263–265.

Liu, K., Kozono, D., Kato, Y., Agre, P., Hazama, A. & Yasui, M. (2005). Conversion of aquaporin 6 from an anion channel to a water-selective channel by a single amino acid substitution. *Proceedings of the National Academy of Sciences USA* **102**, 2192–2197.

Liu, Z., Shen, J., Carbrey, J. M., Mukhopadhyay, R., Agre, P. & Rosen, B. P. (2002). Arsenite transport by mammalian aquaglyceroporins AQP7 and AQP9. *Proceedings of the National Academy of Sciences USA* **99**, 6053–6058.

Lu, M., Lee, M. D., Smith, B. L., Jung, J. S., Agre, P., Verdijk, M. A., Merkx, G., Rijss, J. P. & Deen, P. M. (1996). The human AQP4 gene: definition of the locus encoding two water channel polypeptides in brain. *Proceedings of the National Academy of Sciences USA* **93**, 10908–10912.

Ma, T., Yang, B. & Verkman, A. S. (1997). Cloning of a novel water and urea-permeable aquaporin from mouse expressed strongly in colon, placenta, liver, and heart. *Biochemical and Biophysical Research Communications* **240**, 324–328.

Macey, R. I. (1984). Transport of water and urea in red blood cells. *American Journal of Physiology* **246**, C195–203.

Marinelli, R. A., Pham, L., Agre, P. & LaRusso, N. F. (1997). Secretin promotes osmotic water transport in rat cholangiocytes by increasing aquaporin-1 water

channels in plasma membrane. Evidence for a secretin-induced vesicular translocation of aquaporin-1. *Journal of Biological Chemistry* **272**, 12984–12988.

Marinelli, R. A., Tietz, P. S., Caride, A. J., Huang, B. Q. & LaRusso, N. F. (2003). Water transporting properties of hepatocyte basolateral and canalicular plasma membrane domains. *Journal of Biological Chemistry* **278**, 43157–43162.

Marinelli, R. A., Tietz, P. S., Pham, L. D., Rueckert, L., Agre, P. & LaRusso, N. F. (1999). Secretin induces the apical insertion of aquaporin-1 water channels in rat cholangiocytes. *American Journal of Physiology* **276**, G280–286.

Mathias, R. T., Riquelme, G. & Rae, J. L. (1991). Cell to cell communication and pH in the frog lens. *Journal of General Physiology* **98**, 1085–1103.

Matsuzaki, T., Tajika, Y., Tserentsoodol, N., Suzuki, T., Aoki, T., Hagiwara, H. & Takata, K. (2002). Aquaporins: a water channel family. *Anatomical Science International* **77**, 85–93.

Maurel, C., Reizer, J., Schroeder, J. I., Chrispeels, M. J. & Saier Jr., M. H. (1994). Functional characterization of the Escherichia coli glycerol facilitator, GlpF, in Xenopus oocytes. *Journal of Biological Chemistry* **269**, 11869–11872.

Mitra, A. K., van Hoek, A. N., Wiener, M. C., Verkman, A. S. & Yeager, M. (1995). The CHIP28 water channel visualized in ice by electron crystallography. *Nature Structural Biology* **2**, 726–729.

Mitra, A. K., Yeager, M., van Hoek, A. N., Wiener, M. C. & Verkman, A. S. (1994). Projection structure of the CHIP28 water channel in lipid bilayer membranes at 12-Å resolution. *Biochemistry* **33**, 12735–12740.

Mitsuoka, K., Murata, K., Walz, T., Hirai, T., Agre, P., Heymann, J. B., Engel, A. & Fujiyoshi, Y. (1999). The structure of aquaporin-1 at 4.5-Å resolution reveals short a-helices in the center of the monomer. *Journal of Structural Biology* **128**, 34–43.

Morgan, T. & Berliner, R. W. (1968). Permeability of the loop of Henle, vasa recta, and collecting duct to water, urea, and sodium. *American Journal of Physiology* **215**, 108–115.

Morishita, Y., Sakube, Y., Sasaki, S. & Ishibashi, K. (2004). Molecular mechanisms and drug development in aquaporin water channel diseases: aquaporin superfamily (superaquaporins): expansion of aquaporins restricted to multicellular organisms. *Journal of Pharmacological Science* **96**, 276–279.

Mulders, S. M., Preston, G. M., Deen, P. M., Guggino, W. B., van Os, C. H. & Agre, P. (1995). Water channel properties of major intrinsic protein of lens. *Journal of Biological Chemistry* **270**, 9010–9016.

Murata, K., Mitsuoka, K., Hirai, T., Walz, T., Agre, P., Heymann, J. B., Engel, A. & Fujiyoshi, Y. (2000). Structural determinants of water permeation through aquaporin-1. *Nature* **407**, 599–605.

Nemeth-Cahalan, K. L. & Hall, J. E. (2000). pH and calcium regulate the water permeability of aquaporin 0. *Journal of Biological Chemistry* **275**, 6777–6782.

Nemeth-Cahalan, K. L., Kalman, K. & Hall, J. E. (2004). Molecular basis of pH and Ca^{2+} regulation of aquaporin water permeability. *Journal of General Physiology* **123**, 573–580.

Nguyen, M. K., Nielsen, S. & Kurtz, I. (2003). Molecular pathogenesis of nephrogenic diabetes insipidus. *Clinical and Experimental Nephrology* **7**, 9–17.

Nielsen, S., Chou, C. L., Marples, D., Christensen, E. I., Kishore, B. K. & Knepper, M. A. (1995). Vasopressin increases water permeability of kidney collecting duct by inducing translocation of aquaporin-CD water channels to plasma membrane. *Proceedings of the National Academy of Sciences USA* **92**, 1013–1017.

Nielsen, S., King, L. S., Christensen, B. M. & Agre, P. (1997b). Aquaporins in complex tissues. II. Subcellular distribution in respiratory and glandular tissues of rat. *American Journal of Physiology* **273**, C1549–1561.

Nielsen, S., Nagelhus, E. A., Amiry-Moghaddam, M., Bourque, C., Agre, P. & Ottersen, O. P. (1997a). Specialized membrane domains for water transport in glial cells: high-resolution immunogold cytochemistry of aquaporin-4 in rat brain. *Journal of Neuroscience* **17**, 171–180.

Nollert, P., Harries, W. E., Fu, D., Miercke, L. J. & Stroud, R. M. (2001). Atomic structure of a glycerol channel and implications for substrate permeation in aqua(glycero)porins. *FEBS Letters* **504**, 112–117.

Notredame, C., Higgins, D. & Heringa, J. (2000). T-Coffee: a novel method for multiple sequence alignments. *Journal of Molecular Biology* **302**, 205–217.

Palanivelu, D. V., Kozono, D. E., Engel, A., Suda, K., Lustig, A., Agre, P. & Schirmer, T. (2006). Co-axial association of recombinant eye lens aquaporin-0 observed in loosely packed 3D crystals. *Journal of Molecular Biology* **355**, 605–611.

Pao, G. M., Wu, L. F., Johnson, K. D., Hofte, H., Chrispeels, M. J., Sweet, G., Sandal, N. N. & Saier Jr., M. H. (1991). Evolution of the MIP family of integral membrane transport proteins. *Molecular Microbiology* **5**, 33–37.

Patil, R. V., Han, Z. & Wax, M. B. (1997). Regulation of water channel activity of aquaporin 1 by arginine vasopressin and atrial natriuretic peptide. *Biochemical and Biophysical Research Communications* **238**, 392–396.

Pomes, R. & Roux, B. (1996). Structure and dynamics of a proton wire: a theoretical study of H^+ translocation along the single-file water chain in the gramicidin A channel. *Biophysical Journal* **71**, 19–39.

Pomes, R. & Roux, B. (1998). Free energy profiles for H^+ conduction along hydrogen-bonded chains of water molecules. *Biophysical Journal* **75**, 33–40.

Preston, G. M., Carroll, T. P., Guggino, W. B. & Agre, P. (1992). Appearance of water channels in Xenopus

oocytes expressing red cell CHIP28 protein. *Science* **256**, 385–387.

Preston, G. M., Jung, J. S., Guggino, W. B. & Agre, P. (1993). The mercury-sensitive residue at cysteine 189 in the CHIP28 water channel. *Journal of Biological Chemistry* **268**, 17–20.

Preston, G. M., Jung, J. S., Guggino, W. B. & Agre, P. (1994). Membrane topology of aquaporin CHIP. Analysis of functional epitope-scanning mutants by vectorial proteolysis. *Journal of Biological Chemistry* **269**, 1668–1673.

Raina, S., Preston, G. M., Guggino, W. B. & Agre, P. (1995). Molecular cloning and characterization of an aquaporin cDNA from salivary, lacrimal, and respiratory tissues. *Journal of Biological Chemistry* **270**, 1908–1912.

Rapaport, D., Neupert, W. & Lill, R. (1997). Mitochondrial protein import. Tom40 plays a major role in targeting and translocation of preproteins by forming a specific binding site for the presequence. *Journal of Biological Chemistry* **272**, 18725–18731.

Rash, J. E., Yasumura, T., Hudson, C. S., Agre, P. & Nielsen, S. (1998). Direct immunogold labeling of aquaporin-4 in square arrays of astrocyte and ependymocyte plasma membranes in rat brain and spinal cord. *Proceedings of the National Academy of Sciences USA* **95**, 11981–11986.

Ren, G., Reddy, V. S., Cheng, A., Melnyk, P. & Mitra, A. K. (2001). Visualization of a water-selective pore by electron crystallography in vitreous ice. *Proceedings of the National Academy of Sciences USA* **98**, 1398–1403.

Rich, G. T., Sha'afi, I., Romualdez, A. & Solomon, A. K. (1968). Effect of osmolality on the hydraulic permeability coefficient of red cells. *Journal of General Physiology* **52**, 941–954.

Roy, D., Spector, A. & Farnsworth, P. N. (1979). Human lens membrane: comparison of major intrinsic polypeptides from young and old lenses isolated by a new methodology. *Experimental Eye Research* **28**, 353–358.

Saito, T., Ishikawa, S. E., Sasaki, S., Fujita, N., Fushimi, K., Okada, K., Takeuchi, K., Sakamoto, A., Ookawara, S., Kaneko, T. & Marumo, F. (1997). Alteration in water channel AQP-2 by removal of AVP stimulation in collecting duct cells of dehydrated rats. *American Journal of Physiology* **272**, F183–191.

Sarfaraz, D. & Fraser, C. L. (1999). Effects of arginine vasopressin on cell volume regulation in brain astrocyte in culture. *American Journal of Physiology* **276**, E596–601.

Savage, D. F., Egea, P. F., Robles-Colmenares, Y., O'Connell 3rd, J. D. & Stroud, R. M. (2003). Architecture and selectivity in aquaporins: 2.5 Å X-ray structure of aquaporin Z. *Public Library of Science Biology* **1**, E72.

Shi, L. B., Skach, W. R. & Verkman, A. S. (1994). Functional independence of monomeric CHIP28 water channels revealed by expression of wild-type mutant heterodimers. *Journal of Biological Chemistry* **269**, 10417–10422.

Sidel, V. W. & Solomon, A. K. (1957). Entrance of water into human red cells under an osmotic pressure gradient. *Journal of General Physiology* **41**, 243–257.

Smith, B. L. & Agre, P. (1991). Erythrocyte Mr 28,000 transmembrane protein exists as a multisubunit oligomer similar to channel proteins. *Journal of Biological Chemistry* **266**, 6407–6415.

Smith, D. R., Doucette-Stamm, L. A., Deloughery, C., Lee, H., Dubois, J., Aldredge, T., Bashirzadeh, R., Blakely, D., Cook, R., Gilbert, K., Harrison, D., Hoang, L., Keagle, P., Lumm, W., Pothier, B., Qiu, D., Spadafora, R., Vicaire, R., Wang, Y., Wierzbowski, J., Gibson, R., Jiwani, N., Caruso, A., Bush, D., Reeve, J. N., *et al.* (1997). Complete genome sequence of Methanobacterium thermoautotrophicum deltaH: functional analysis and comparative genomics. *Journal of Bacteriology* **179**, 7135–7155.

Solomon, A. K., Chasan, B., Dix, J. A., Lukacovic, M. F., Toon, M. R. & Verkman, A. S. (1983). The aqueous pore in the red cell membrane: band 3 as a channel for anions, cations, nonelectrolytes, and water. *Annals of the New York Academy of Sciences* **414**, 97–124.

Strange, K., Willingham, M. C., Handler, J. S. & Harris Jr., H. W. (1988). Apical membrane endocytosis via coated pits is stimulated by removal of antidiuretic hormone from isolated, perfused rabbit cortical collecting tubule. *Journal of Membrane Biology* **103**, 17–28.

Stroud, R. M., Miercke, L. J., O'Connell, J., Khademi, S., Lee, J. K., Remis, J., Harries, W., Robles, Y. & Akhavan, D. (2003a). Glycerol facilitator GlpF and the associated aquaporin family of channels. *Current Opinion in Structural Biology* **13**, 424–431.

Stroud, R. M., Savage, D., Miercke, L. J., Lee, J. K., Khademi, S. & Harries, W. (2003b). Selectivity and conductance among the glycerol and water conducting aquaporin family of channels. *FEBS Letters* **555**, 79–84.

Sui, H., Han, B. G., Lee, J. K., Walian, P. & Jap, B. K. (2001). Structural basis of water-specific transport through the AQP1 water channel. *Nature* **414**, 872–878.

Tajkhorshid, E., Nollert, P., Jensen, M. O., Miercke, L. J., O'Connell, J., Stroud, R. M. & Schulten, K. (2002). Control of the selectivity of the aquaporin water channel family by global orientational tuning. *Science* **296**, 525–530.

Takemoto, L., Takehana, M. & Horwitz, J. (1986). Covalent changes in MIP26K during aging of the human lens membrane. *Investigative Ophthalmology and Visual Sciences* **27**, 443–446.

Tornroth-Horsefield, S., Wang, Y., Hedfalk, K., Johanson, U., Karlsson, M., Tajkhorshid, E., Neutze, R. & Kjellbom, P. (2006). Structural mechanism of plant aquaporin gating. *Nature* **439**, 688–694.

Tournaire-Roux, C., Sutka, M., Javot, H., Gout, E., Gerbeau, P., Luu, D. T., Bligny, R. & Maurel, C.

(2003). Cytosolic pH regulates root water transport during anoxic stress through gating of aquaporins. *Nature* **425**, 393–397.

Tsukaguchi, H., Shayakul, C., Berger, U. V., Mackenzie, B., Devidas, S., Guggino, W. B., van Hoek, A. N. & Hediger, M. A. (1998). Molecular characterization of a broad selectivity neutral solute channel. *Journal of Biological Chemistry* **273**, 24737–24743.

Ussing, H. H. (1965). Transport of electrolytes and water across epithelia. *Harvey Lecture* **59**, 1–30.

Varadaraj, K., Kumari, S., Shiels, A. & Mathias, R. T. (2005). Regulation of aquaporin water permeability in the lens. *Investigative Ophthalmology and Visual Sciences* **46**, 1393–1402.

Varadaraj, K., Kushmerick, C., Baldo, G. J., Bassnett, S., Shiels, A. & Mathias, R. T. (1999). The role of MIP in lens fiber cell membrane transport. *Journal of Membrane Biology* **170**, 191–203.

Verkman, A. S. (2005). More than just water channels: unexpected cellular roles of aquaporins. *Journal of Cell Science* **118**, 3225–3232.

Wade, J. B., Stetson, D. L. & Lewis, S. A. (1981). ADH action: evidence for a membrane shuttle mechanism. *Annals of the New York Academy of Sciences* **372**, 106–117.

Walz, T., Hirai, T., Murata, K., Heymann, J. B., Mitsuoka, K., Fujiyoshi, Y., Smith, B. L., Agre, P. & Engel, A. (1997). The three-dimensional structure of aquaporin-1. *Nature* **387**, 624–627.

Walz, T., Smith, B. L., Agre, P. & Engel, A. (1994b). The three-dimensional structure of human erythrocyte aquaporin CHIP. *EMBO Journal* **13**, 2985–2993.

Walz, T., Smith, B. L., Zeidel, M. L., Engel, A. & Agre, P. (1994a). Biologically active two-dimensional crystals of aquaporin CHIP. *Journal of Biological Chemistry* **269**, 1583–1586.

Walz, T., Typke, D., Smith, B. L., Agre, P. & Engel, A. (1995). Projection map of aquaporin-1 determined by electron crystallography. *Nature Structural Biology* **2**, 730–732.

Wang, Y., Schulten, K. & Tajkhorshid, E. (2005). What makes an aquaporin a glycerol channel? A comparative study of AqpZ and GlpF. *Structure* **13**, 1107–1118.

Wistow, G. J., Pisano, M. M. & Chepelinsky, A. B. (1991). Tandem sequence repeats in transmembrane channel proteins. *Trends in Biochemical Sciences* **16**, 170–171.

Yang, B. & Verkman, A. S. (1997). Water and glycerol permeabilities of aquaporins 1-5 and MIP determined quantitatively by expression of epitope-tagged constructs in Xenopus oocytes. *Journal of Biological Chemistry* **272**, 16140–16146.

Yano, M., Marinelli, R. A., Roberts, S. K., Balan, V., Pham, L., Tarara, J. E., de Groen, P. C. & LaRusso, N. F. (1996). Rat hepatocytes transport water mainly via a non-channel-mediated pathway. *Journal of Biological Chemistry* **271**, 6702–6707.

Yasui, M., Hazama, A., Kwon, T. H., Nielsen, S., Guggino, W. B. & Agre, P. (1999a). Rapid gating and anion permeability of an intracellular aquaporin. *Nature* **402**, 184–187.

Yasui, M., Kwon, T. H., Knepper, M. A., Nielsen, S. & Agre, P. (1999b). Aquaporin-6: an intracellular vesicle water channel protein in renal epithelia. *Proceedings of the National Academy of Sciences USA* **96**, 5808–5813.

Zampighi, G., Simon, S. A., Robertson, J. D., McIntosh, T. J. & Costello, M. J. (1982). On the structural organization of isolated bovine lens fiber junctions. *Journal of Cell Biology* **93**, 175–189.

Zampighi, G. A., Hall, J. E., Ehring, G. R. & Simon, S. A. (1989). The structural organization and protein composition of lens fiber junctions. *Journal of Cell Biology* **108**, 2255–2275.

Zampighi, G. A., Hall, J. E. & Kreman, M. (1985). Purified lens junctional protein forms channels in planar lipid films. *Proceedings of the National Academy of Sciences USA* **82**, 8468–8472.

Zeidel, M. L., Ambudkar, S. V., Smith, B. L. & Agre, P. (1992). Reconstitution of functional water channels in liposomes containing purified red cell CHIP28 protein. *Biochemistry* **31**, 7436–7440.

Zeidel, M. L., Nielsen, S., Smith, B. L., Ambudkar, S. V., Maunsbach, A. B. & Agre, P. (1994). Ultrastructure, pharmacologic inhibition, and transport selectivity of aquaporin channel-forming integral protein in proteoliposomes. *Biochemistry* **33**, 1606–1615.

Zelenina, M., Zelenin, S., Bondar, A. A., Brismar, H. & Aperia, A. (2002). Water permeability of aquaporin-4 is decreased by protein kinase C and dopamine. *American Journal of Physiology. Renal Physiology* **283**, F309–318.

Zeuthen, T. & Klaerke, D. A. (1999). Transport of water and glycerol in aquaporin 3 is gated by H^+. *Journal of Biological Chemistry* **274**, 21631–21636.

Zhang, R., van Hoek, A. N., Biwersi, J. & Verkman, A. S. (1993a). A point mutation at cysteine 189 blocks the water permeability of rat kidney water channel CHIP28k. *Biochemistry* **32**, 2938–2941.

Zhang, R., Skach, W., Hasegawa, H., van Hoek, A. N. & Verkman, A. S. (1993b). Cloning, functional analysis and cell localization of a kidney proximal tubule water transporter homologous to CHIP28. *Journal of Cell Biology* **120**, 359–369.

Zhang, R. B., Logee, K. A. & Verkman, A. S. (1990). Expression of mRNA coding for kidney and red cell water channels in Xenopus oocytes. *Journal of Biological Chemistry* **265**, 15375–15378.